APPLICATION OF MULTI-SEGMENT ARPS HYPERBOLIC DECLINE MODEL BASED ON IDENTIFIED FLOW REGIMES IN UNCONVENTIONAL WELLS

A Thesis

by

BYRON CASEY SHERMAN

Submitted to the Office of Graduate and Professional Studies of
Texas A&M University
in partial fulfillment of the requirements for the degree of

MASTER OF SCIENCE

Chair of Committee,	W. John Lee
Committee Members,	John Jochen
	Derya Akleman
Head of Department,	Jeff Spath

December 2019

Major Subject: Petroleum Engineering

ABSTRACT

Unconventional reservoirs, specifically volatile oil shale plays, behave with much more complexity than conventional reservoirs and cannot be modeled consistently and accurately with Arps methods. An adaptation of the Arps method has been suggested as a viable method to accurately model the decline of a volatile oil shale well. This method applies the Arps hyperbolic decline model using multiple segments across the life of the well based on distinct flow regimes identified in the well's production history. Modeling multiple segments based on flow regimes observed in production data adds a degree of ingenuity and robustness to the widely accepted traditional Arps model. The objective of this research project is to learn how to effectively apply multi-segment Arps hyperbolic decline models to horizontal, multi-fractured volatile oil wells in the Permian Basin.

The Multi-Segment Hyperbolic Decline Model is a viable method in forecasting the decline of unconventional wells. The transient nature of ultra-low permeability shale reservoirs indicates a more complex decline profile than can be modeled successfully using the modified Arps model. Typical volatile oil shale wells are characterized by steep initial declines that gradually level off as the well transitions from transient linear flow to boundary dominated flow. The resulting decline profile segmented by distinct flow regimes results in an estimated ultimate recovery that is greater than that of the modified Arps model, suggesting the Arps model is underestimating reserves when compared to the multi-segment method.

CONTRIBUTORS AND FUNDING SOURCES

Contributors

This work was supervised by a thesis committee consisting of Professor W. John Lee and John Jochen of the Department of Petroleum Engineering and Professor Derya Akleman of the Department of Statistics.

All other work conducted for the thesis was completed independently by the student.

Funding

There are no outside funding contributions to acknowledge related to the research and compilation of this document.

TABLE OF CONTENTS

LIST OF FIGURES

FIGURE Page

LIST OF TABLES

TABLE Page

INTRODUCTION

Modeling Conventional Wells Using Arps Method

Conventional reservoirs have been accurately and easily modeled with Arps decline models industry-wide since at least 1945. Arps defines the decline behavior of a well using an initial production rate (q_i), initial decline rate (D_i), and decline exponent factor (b). The model further categorizes a well into exponential ($b = 0$), hyperbolic ($b > 0$, b not equal to 1), or harmonic ($b = 1$) declines based on the behavior of the well (Arps 1945). Arps' exponential, hyperbolic, and harmonic equations are presented below as **Eq. 1**, **2**, and **3**, respectively. The most commonly used modified Arps model assumes a hyperbolic decline with a constant b-factor throughout the life of the well and incorporates a terminal decline rate that switches the model to exponential decline when the terminal decline rate is reached. The Arps model assumes boundary dominated flow (BDF), meaning flow from the reservoir is influenced by the boundary of the reservoir or nearby wells as seen in **Fig. 1**. The Arps hyperbolic decline model has proved successful, accurate, and simple in modeling conventional reservoir decline; it is the industry standard when it comes to modeling conventional reservoirs.

$$q(t) = \frac{q_i}{e^{D_i t}} \quad \text{.....(1)}$$

$$q(t) = \frac{q_i}{(1+bD_i t)^{1/b}} \quad \text{.....(2)}$$

$$q(t) = \frac{q_i}{1+D_i t} \quad \text{.....(3)}$$

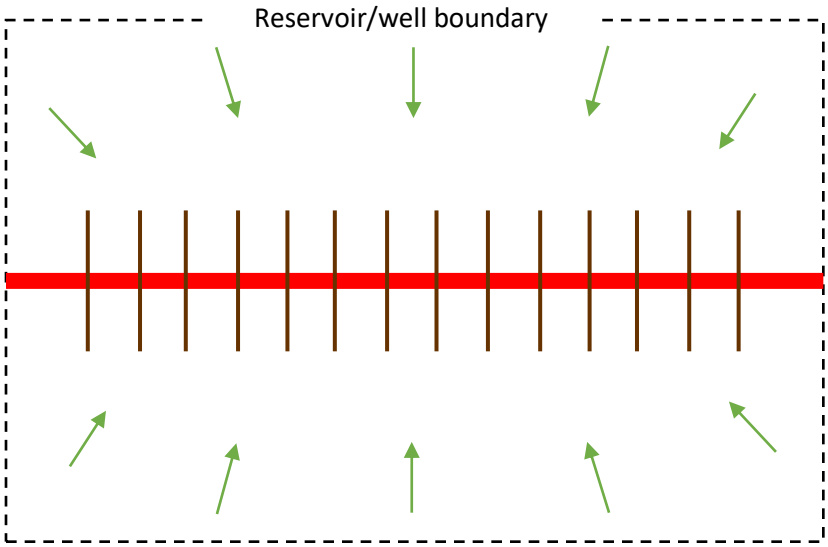

Fig. 1—Boundary dominated flow due to well interference.

Modeling Unconventional Wells Using Arps Method

Unconventional reservoirs, however, behave with much more complexity than conventional reservoirs and cannot be modeled as easily and accurately with conventional methods. Whereas conventional wells exist in BDF for the majority of the life of the well, unconventional wells exist in transient linear flow (LF) for months to years before transitioning to BDF (Wattenbarger et al. 1998). This indicates that unconventional reservoirs do not show reservoir boundary effects for many years due to the ultra-low permeability often present in unconventional plays. Early production from these wells results from matrix drainage linearly into natural and/or hydraulic fractures **(Fig. 2)** and then to the wellbore rather than radially from the full extent of the reservoir. Since the Arps decline model is based on the BDF assumption, unconventional reservoirs cannot be accurately forecasted using this method. Modeling the decline of unconventional wells in transient linear flow becomes much more complicated than conventional wells in radial or boundary dominated flow. A horizontal, fractured, ultra-low

permeability well is expected to exist in LF for many months to years before a transitioning to BDF. Theoretically, using Arps hyperbolic decline, true linear flow is best modeled with a b-factor of 2.0 (Spivey et al. 2001). In reality, variables such as operational conditions, well spacing, reservoir heterogeneity, completion efficiency, and particularly fracture interference cause wells producing in LF to be best fit with b-factors ranging from 1.5 to 2.0. For example, increasing completion efficiency, specifically fracture length, causes the b-factor to decrease from 2.0 (Kupchenko et al. 2008). This study assumes LF is defined by this b-factor range of 1.5 to 2.0 rather than the true LF b-factor of 2.

Although unconventional wells are believed to flow linearly for months to years, a well will eventually transition to flow that is affected by complete fracture interference. The transition phase could possibly be seen in well production data, but the boundary dominated flow regime is not likely to be seen due to insufficiently long production histories currently available. As this transition occurs, the b-factor has been observed as not constant as suggested by the Arps model (Varma et al. 2018). In fact, the b-factor in unconventional reservoirs declines over time as the well transitions from LF to BDF. We estimate the b-factor of the transition zone ranges from 0.5 to 1.5. A solution-gas-drive well producing in BDF is expected to be fit best with a b-factor of 0.3 (Fetkovich 1996). Furthermore, hyperbolic decline b-factors cannot exceed one for the entire life of a well because this yields an estimate of infinite reserves (totally unrealistic) and generally causes an overestimation of ultimate recovery. The declining nature of the b-factor as the reservoir flow moves from LF to BDF renders the modified Arps model inaccurate and misused in unconventional reservoirs. A constant b-factor Arps hyperbolic decline model cannot accurately model the decline of unconventional reservoirs.

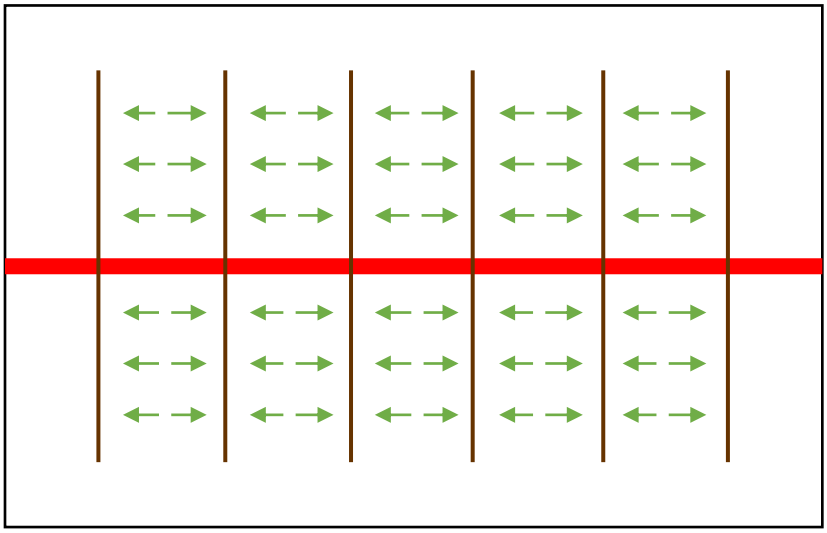

Fig. 2—Linear flow.

Modeling Unconventional Wells Using New Methods

Researchers have suggested that newer decline models, such as Duong, power law exponential, etc., may better represent the complicated decline of volatile oil shale reservoirs. The Duong (2011) model assumes long term linear flow and often overestimates reserves. Ilk et al. 2008 proposed the power law exponential model that can be flexible enough to incorporate LF and BDF regimes for shale gas reservoirs. The added complexity, limitations, and lack of knowledge of these models make it challenging for their widespread acceptance as accurate and suitable long-term models for forecasting the decline of shale reservoirs (Makinde and Lee 2016). With its simplicity and accuracy in forecasting wells for nearly a hundred years, the Arps hyperbolic decline remains the most accepted and long-standing method to forecast the decline of a well, conventional or unconventional. However, the model simplicity, subjectivity, and inaccuracies in modeling unconventional wells calls for the need to adapt the model to better fit unconventional wells. To adapt this model to make it more suitable for unconventional reservoirs, hybrid Arps models have been suggested. The Multi-Segment Hyperbolic (MSH)

model, exemplified in **Fig. 3,** follows the Arps hyperbolic equation (Eq. 2 above) but incorporates multiple segments of hyperbolic declines based on the distinct flow regimes observed in production data (Jeyachandra et al. 2016). This method utilizes the simplicity and popularity of the modified Arps model but adds robustness by segmenting the production data into the observed flow regimes, most often transient LF, partial fracture interference, transition to BDF, and BDF (Varma et al. 2018).

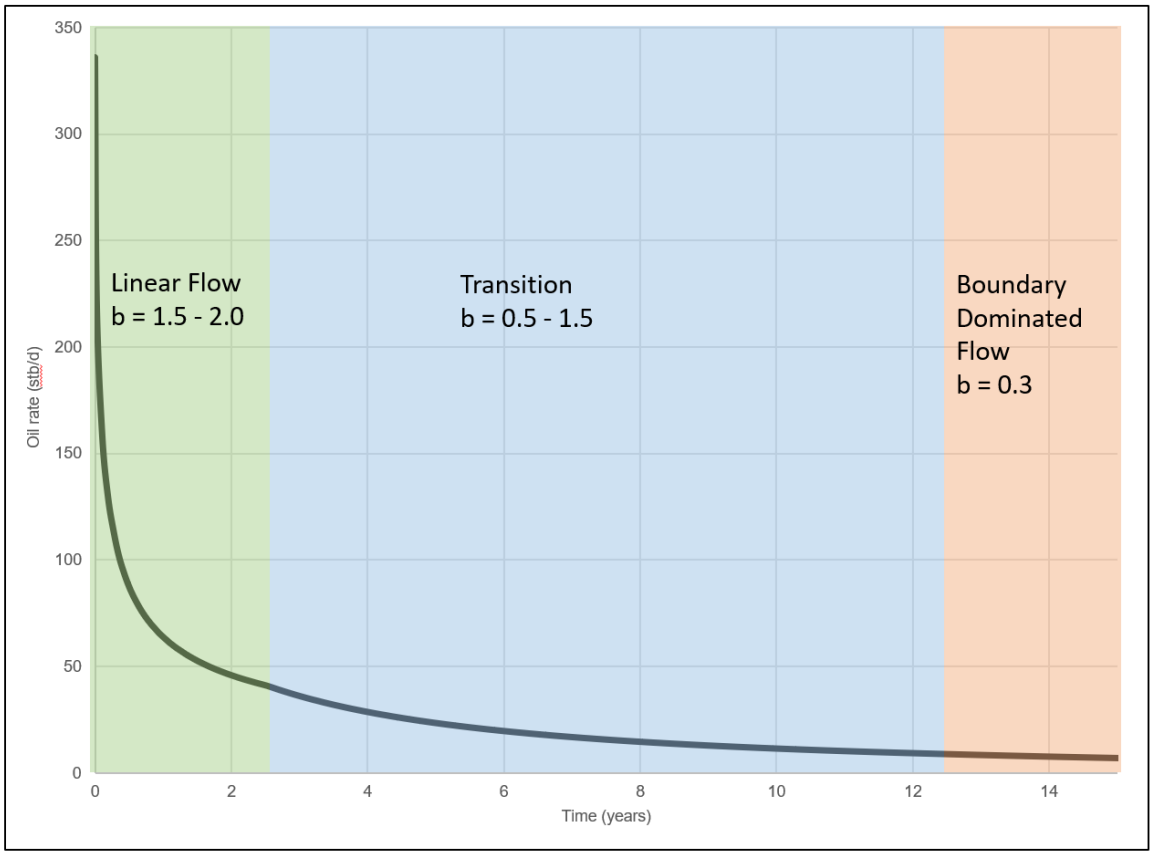

Fig. 3—Example of a multi-segment hyperbolic decline model based on LF, transition to BDF, and BDF segments.

Reserves estimation is an important part of the oil and gas industry. Estimating the reserves for a reservoir impacts business management, accounting, financing, and government regulation (Abdel, Mawla and Hegazy 2015). Over or under-estimating reserves can negatively impact business development and can even cause legal implications for a company (Olson et al. 2019). As horizontal, hydraulically fractured shale wells become the focal point of today's oil and gas industry, better understanding of how to forecast unconventional wells is needed to ensure reserves estimation is done quickly, consistently, and accurately. Hybrid models, like the MSH method, are gaining traction as the industry recognizes the limitations of conventional forecasting methods in unconventional plays.

This study serves to effectively apply the multi-segment hyperbolic method to a 100-well data set of horizontal, hydraulically fractured, volatile oil shale wells in the Permian Basin and compare the resulting decline models to modified Arps decline curves. It also serves to gain further insight into long-term volatile oil shale well behavior. Specifically, the following objectives will be achieved through this study:

1. Identify distinct flow regimes in well production data using diagnostic tools.
2. Generate MSH decline models for each well based on identified flow regimes.
3. Generate MSH type wells.
4. Generate modified Arps hyperbolic decline models for each well.
5. Generate modified Arps hyperbolic type wells.

Literature Review of Flow Regimes

Bilinear Flow

Bilinear flow (BLF) is characterized by hydrocarbon flow linearly both within the fracture and within the formation, illustrated in **Fig. 4**. It is possible but not likely to observe BLF in early time in unconventional wells and if observed, it is typically brief. Bilinear flow can be falsely identified in very early time as the well is brought online and the fractures are cleaned up, meaning fracture fluid is flowed back to the surface and proppant is set in the fractures. Since it is uncommon, short-lived, and often falsely identified, BLF is typically ignored unless observed for a significant period of time (Kanfar and Alkouh 2014). It is associated with a very high Arps *b* parameter up to 4.0 (Kupchenko et al. 2008).

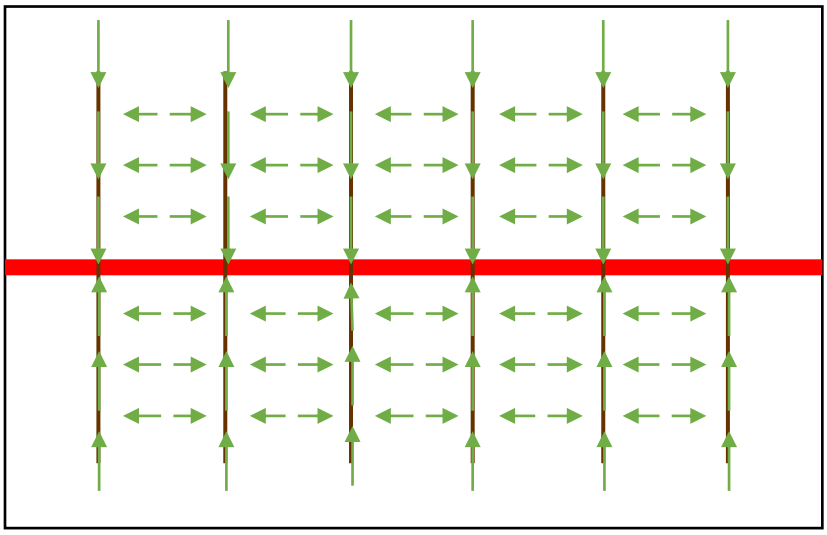

Fig. 4—Bilinear flow.

Linear Flow

Unconventional wells produce hydrocarbons from the stimulated reservoir volume, or the volume of reservoir rock that has been hydraulically fractured to create a network of highly permeable fractures that are conductive of reservoir fluids. The linear flow regime is characterized by hydrocarbon flow linearly and perpendicular to hydraulic fractures, as depicted previously by Fig. 2. The transient linear flow regime is the dominant flow regime in shale wells, lasting months to years (Kupchenko et al. 2008). Linear flow is associated with high *b* parameters from 1.5-2.0.

Partial Fracture Interference

Multiple-well pads and multiple-stage hydraulic fracturing can create partial or complete interconnected fracture networks that induce complex hydrocarbon flow patterns, as depicted by **Fig. 5**. In this case, a well may show pseudo-boundary effects, meaning partial fracture interference creates an impression that the reservoir boundary is influencing the well's production (Tang et al. 2017). Often times this phenomenon can occur almost immediately after the onset of production, meaning the fracture stages are already communicating enough to bypass the LF period and immediately indicate transition-like flow regimes. Wells experiencing partial fracture interference are typically fit without a LF segment and a b-factor from 0.5 -1.5. Note this b-factor range is the same as for the transition phase. These flow regimes are exhibiting the exact same behavior, but partial fracture interference is not preceded by LF, whereas transitional flow is preceded by LF.

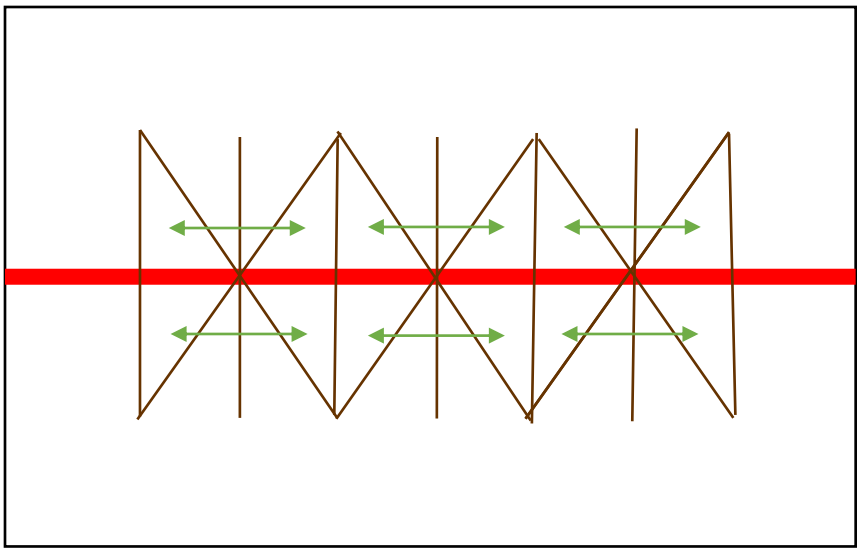

Fig. 5—Partial fracture interference (transition to BDF).

Transition to Boundary-Dominated Flow

Unconventional wells will gradually transition from LF to BDF as the well begins to produce from the complex, interconnected fracture networks rather than linearly in individual fractures (Kupchenko et al. 2008). As more fractures begin to communicate, transitional flow is exhibited, as in Fig. 5 above. This flow regime is exhibiting the same behavior as partial fracture interference, but transitional flow follows LF. The transition flow regime is less likely than LF to be observed in production data due to the long duration of LF as well as the lack of long-term production data. This transition occurs after LF and is associated with a declining b-factor of 0.5-1.5.

Boundary Dominated Flow

An unconventional well will see boundary effects when the well begins to produce entirely from the complex, interconnected fracture network generated through hydraulic fracturing, as seen in **Fig 6**. In conventional wells, BDF can observed for much of the life of the

well. In unconventional wells, however, boundary dominated flow is not observed for a long period of time, if at all, due to the transient nature of the ultra-low permeability reservoirs. Fetkovich (1996) accurately modeled solution-gas-drive volatile oil reservoirs with an Arps *b*-factor of 0.3. This b-factor will be used as the assumed b-factor for all BDF regime decline segments.

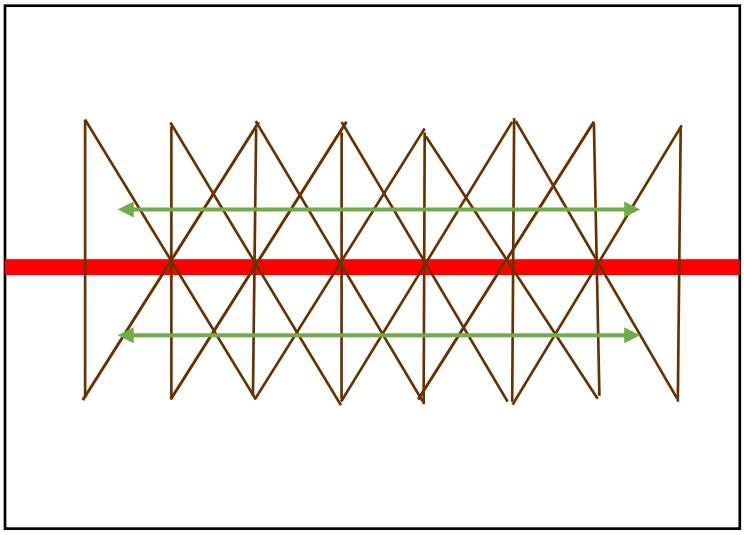

Fig. 6—Boundary dominated flow due to complete fracture interference.

FLOW REGIME ANALYSIS

Overview

Flow regime identification is performed using rate transient analysis incorporating well production and bottom hole pressure data. Rate transient analysis involves the interpretation of this rate and pressure data using diagnostic plots to diagnose reservoir behavior. **Table 1** details a summary of diagnostic plots used to identify flow regimes. **Table 2** summarizes the steps taken in the flow regime identification portion of this analysis. Note that any trendline slope is hereafter referred to as a positive value whereas in actuality the slope is actually negative. For example, a well in LF technically exhibits a -½ slope on a log-log plot of rate vs time, but this study refers to the slope as "½ slope" for simplicity.

Diagnostic Plot	Purpose
1. q vs t	Data correlation and validation
2. p_{wf} vs t	Data correlation and validation
3. Log(q) vs Log(t)	Flow regime identification
4. Log($q/\Delta p$) vs Log(t)	Flow regime identification

Table 1—Diagnostic plots used and their purpose in flow regime analysis.

1. Data quality control (using plots 1 and 2) **a.** Data correlation **b.** Data noise
2. Flow regime identification (using plot 4)
3. Best fit slope and duration of each flow regime recorded

Table 2—Summary of flow regime analysis procedure.

Data Correlation

The rate and pressure data used in this study is real world data from wells in the Wolfcamp and Bone Springs formations in the Permian Basin. The oil rate data provided for this study are daily field measurements that are subject to human or other forms of measurement error. The pressure data provided for this study are daily calculated bottom hole pressures using a surface-to-bottom-hole pressure correlation from measured surface pressure data and individual well and reservoir parameters. These data sets are subject to errors; this can affect the analysis performed. It is important to check the quality of data involved in the analysis to understand the certainty with which conclusions can be drawn (Ilk et al. 2011). The rate, q, and flowing bottom hole pressure, p_{wf}, data were checked using plots 1 and 2 from Table 1 to ensure the data correlated. When any of the wells in the 100-well set were deemed to have invalid data, the wells were removed from the analysis. If the well data was deemed valid, analysis was continued and performed on the well. **Fig. 7** shows a well with invalid data that was removed from the data set. The pressure increases for a significant portion of the production data and segments of this data also have increasing rate. This relationship is not physically possible so the well is removed from the analysis. **Fig. 8** shows a well with valid data that was included in the analysis moving forward. The rate and pressure data for this well correlated and was deemed valid for the analysis. This data correlation analysis was performed on all 100 wells in the data set with only 73 wells being identified has having valid data and thus included in the analysis. This reduced the uncertainty in the results of the analysis as a whole. Two of the wells in the data set, wells 99 and 100, contained both measured rate and pressure data. These well data are the most accurate in the entire data set since the bottom hole pressures were collected using a bottom hole gauge.

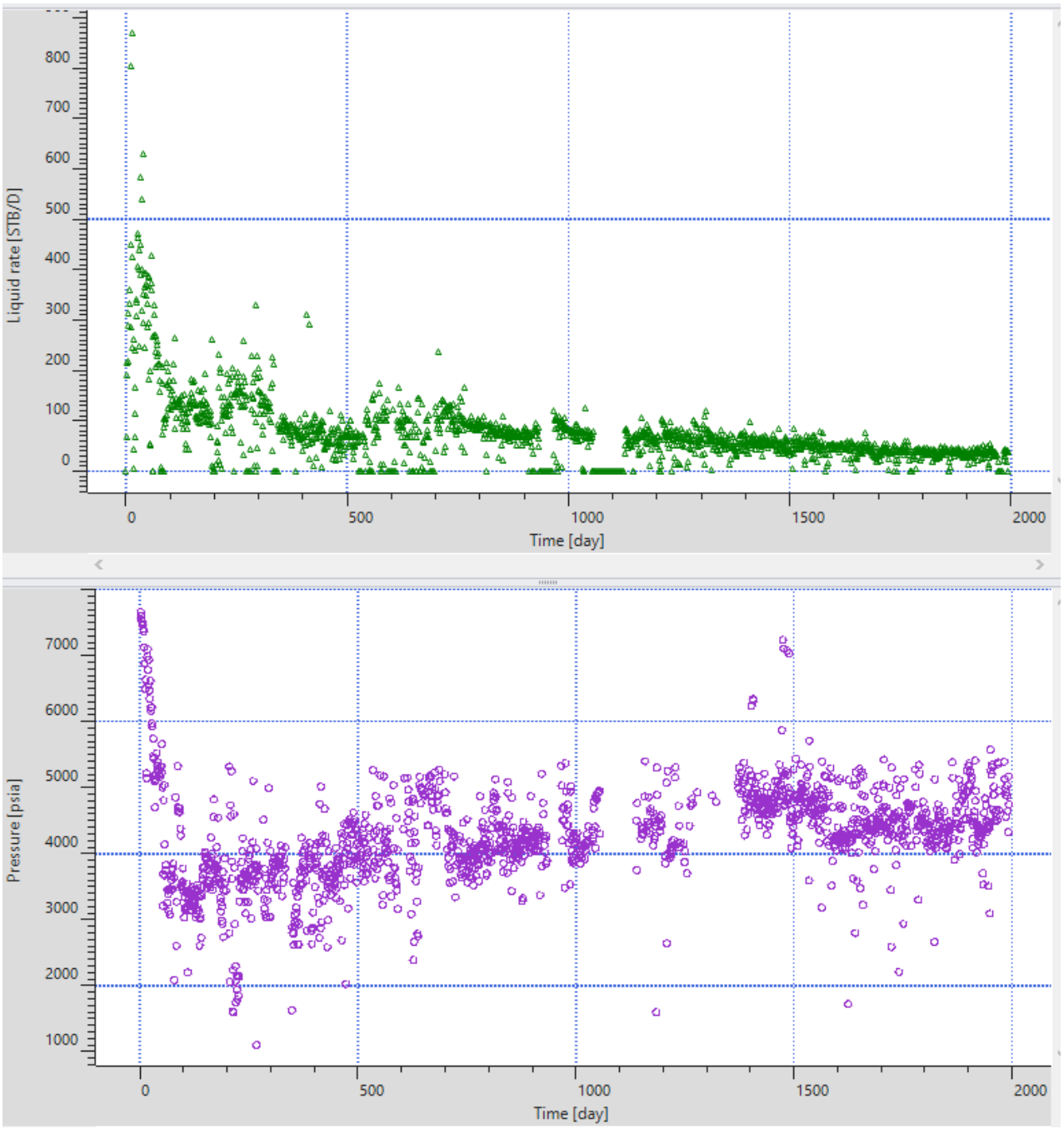

Fig. 7—Example of a well with invalid pressure data that was removed from the analysis.

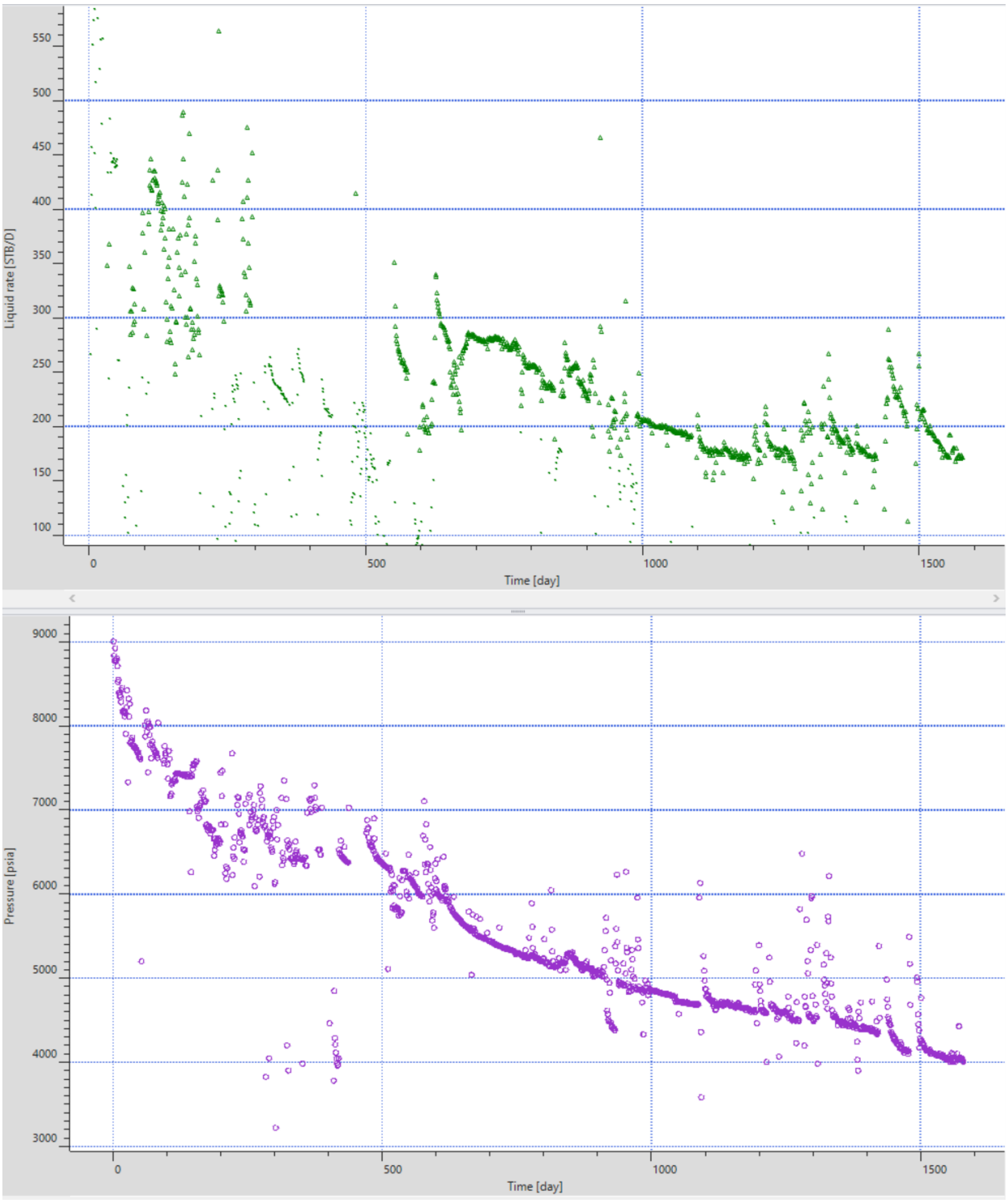

Fig. 8—Example of a well with valid rate and pressure data that was included in the analysis.

Data Noise

Data noise can have a significant impact on flow regime identification and decline curve analysis. Field data is typically associated with disruptions and significant noise throughout the life of the well. Well events such as shut-ins, workovers, choke changes, and other operational changes can disrupt rate data from the decline profile of the well (Chaudhary and Lee 2016). Fracture fluid flowback often dominates the early life of the well due to high production rates of fracture fluids and subsequent lower production rates of reservoir fluids. After the first three to six months of production, the well will usually have completed flowback and established a peak oil rate followed by a decline in production rates. Once this decline has begun, the data becomes valid and usable for flow regime and decline curve analysis. Rate data such as this can be cleaned up using a manual lasso tool to select points which are considered outliers and should be excluded from the data. The manual nature of this tool can create some biases when filtering the data. The more the data is filtered, the less representative of the true reservoir decline the data becomes. It is important to ensure the analysis is unbiased from over data filtering. **Fig. 9** shows an example of a well with significant noise associated with the rate data due to shut-ins and fracture clean-up. Significant noise is also associated with the calculated bottom hole pressure data due to the nature of the calculation. The calculation was performed by an outside party prior to obtaining the data, so some uncertainty as well as noise lies within this calculated data. **Fig. 10** shows an example of a well with significant noise associated with pressure data. The wells in this data set were categorized based on the level of noise seen in the pressure data. Wells with significant noise in the pressure data as in Fig. 10 were labeled “bad data,” whereas wells with little noise in the pressure data, as in Fig. 8, were labeled “good data.” Flow regime and decline curve analysis was performed on wells with both good and bad data noise; however, only the

good data wells were considered for final results and conclusions, since this well category contained the data with the least amount of uncertainty.

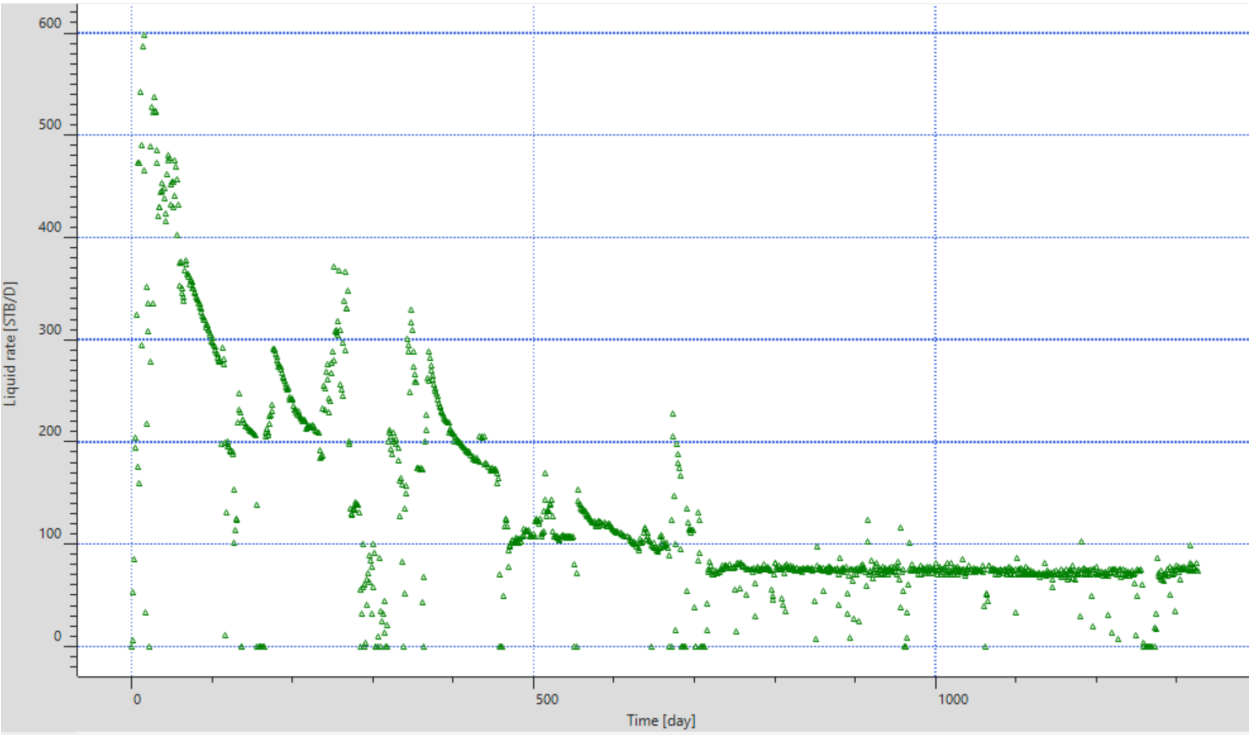

Fig. 9—Example of a well with noisy rate data due to fracture clean-up and frequent shut-ins.

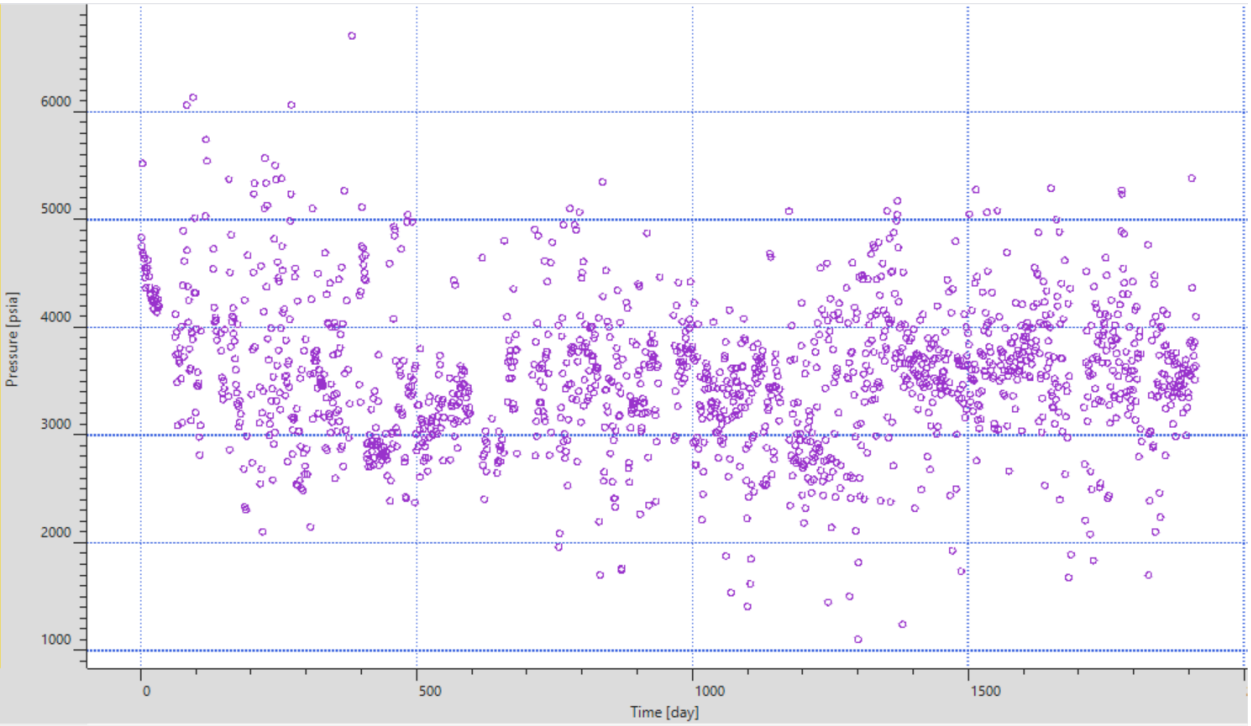

Fig. 10—Example of a well with noisy pressure data, categorized as "bad" data.

Analysis

The flow regimes were identified using plots 3 and 4 in Table 1. Plot 3, log(q) vs log(t), is the plot typically used in the identification of flow regimes in unconventional wells under the assumption that the well is producing at a constant flowing pressure. However, almost all field data exists contains both variable rate and variable pressure. Analyzing only the rate data while assuming constant pressure production can lead to significant errors when identifying the true reservoir signature. In this case, plot 3 cannot be trusted to accurately identify flow regimes for wells with significant data variability. However, use of plot 3 is still a good preliminary tool to check what flow regimes are likely to be seen. The following procedure is useful with plot 3. A straight-line with a ½ slope trend on a log-log plot of rate vs time can indicate the presence of

transient LF. Rate data is significantly affected by well operation condition changes that cause deviations in the ½ slope line despite the well remaining in linear flow. For example, a choke change should cause a straight-line trend deviation as the flow rates and pressures are suddenly shifted, but the overall trend should return to a ½ slope line over time if the well is still in linear flow. It is important to take operational changes into consideration when analyzing production data. This data set did not include operational changes and well events, so deviations in straight line trends were assumed to be due to flow regime shifts as long as the shifted trend did not return to the previous trend. **Fig. 11** is an example of a well that shows ½ slope on plot 3, indicating the well is producing in the LF regime. The fracture clean-up period of the data at early times can clearly be seen on this example. After a couple months of production, the well is clearly trending at ½ slope and can be interpreted as in the LF regime. Use of similar plots incorporating square root time or material balance time can also be used to confirm linear flow, although caution is suggested when using these methods because straight-line trends and deviations from straight line trends can mislead the analyst into believing linear flow exists or deviation form linear flow has occurred when in fact the opposite is true.

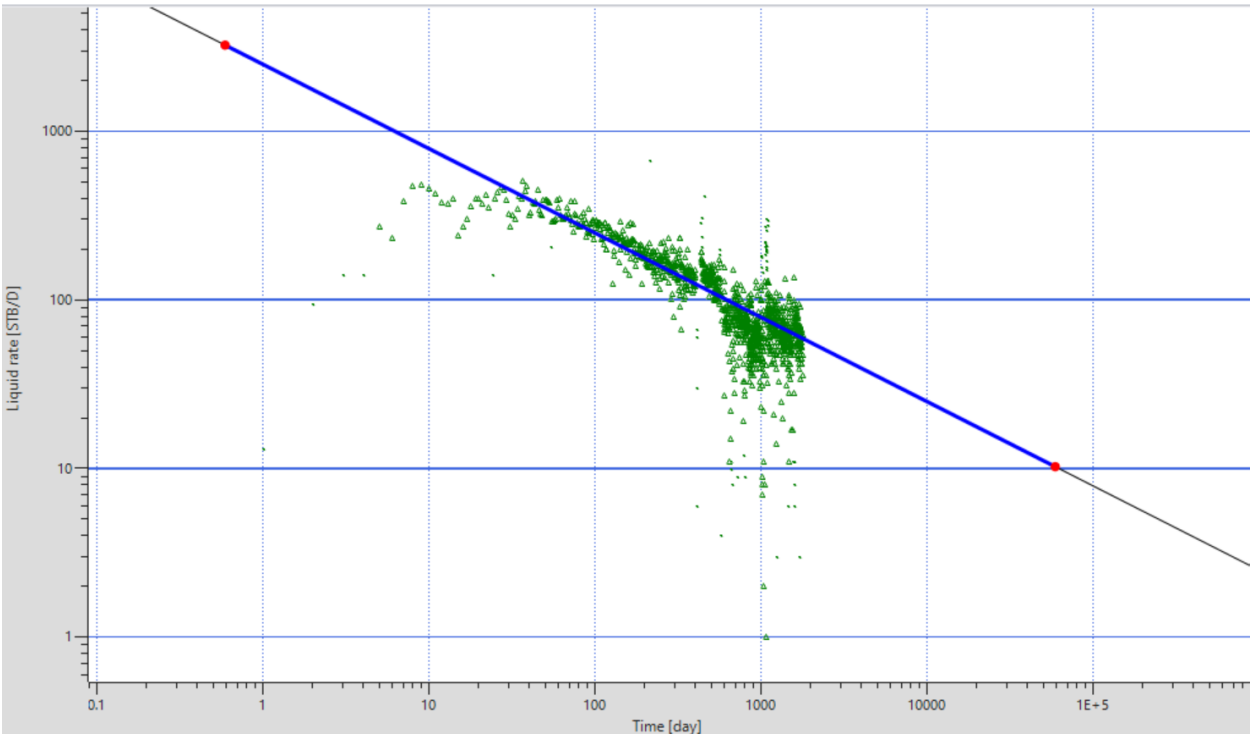

Fig. 11—Example of a well in LF based on the ½ slope on log(q) vs log(t).

To more accurately and consistently identify flow regimes, plot 4 is suggested as a more robust method than plot 3 since this plot normalizes rate using bottom hole pressure data. The pressure-normalized rates (PNR), shown in **Eq. 4**, better represent the true reservoir performance of wells under unstable flowing conditions and allow for more accurate flow regime analysis (Lacayo and Lee 2014). The initial reservoir pressure used in the PNR calculation is subject to uncertainty in this data set. The initial pressure can be roughly estimated using the total vertical depth and **Eq. 5**, but in some cases the initial reservoir pressure estimate was less than some of the calculated bottom hole pressure data points. This is neither feasible or realistic, so the initial pressure estimate for these wells was adjusted to ensure that $p_i > p_{wf}$. However, not all wells had total vertical depth data. For the wells without total vertical depth data, the initial pressure was set at the average initial pressure estimated in the previous steps for each formation. This

remains a source of mild uncertainty in the analysis, but small shift in initial pressure does not have a significant impact on flow regimes analysis. The value of 0.7 psi/ft in Eq. 5 is a pressure gradient estimate obtained for the Permian Basin (Fairhurst et al. 2012). **Fig. 12** shows an example of a well that shows disrupted rate data on plot 3, but once normalized, shows a clear straight-line trend on plot 4. Moving forward, plot 4 is used as the primary diagnostic tool to identify flow regimes. Theoretically, a ½ slope straight line on plot 4 indicates the existence of transient LF. With field data, however, LF will be indicated by straight-line trends that show a slope of about (but not exactly) ½. Unstable operating conditions, well communication, reservoir heterogeneity, and completion efficiency can cause disruptions in the ½ slope trend of field data. For this study, LF was assumed for wells showing slopes of ½ to 2/3. The best fit slope and segment duration of the identified segments of data was recorded for each well.

$$PNR = \frac{q}{\Delta p} = \frac{q}{p_i - p_{wf}} \quad \text{.....(4)}$$

$$p_i \approx TVD\ [ft] * 0.7\ [psi/ft] \quad \text{.....(5)}$$

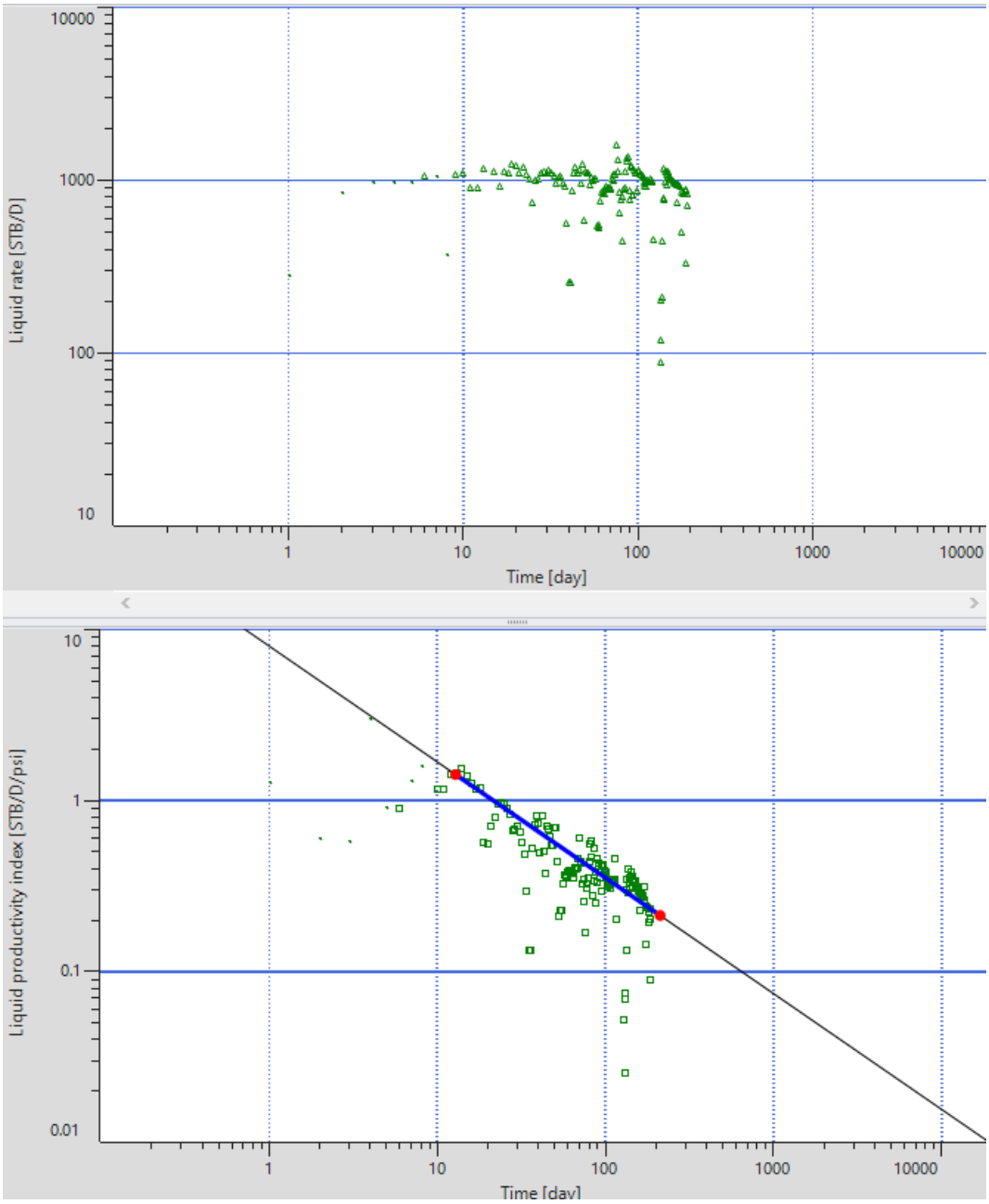

Fig. 12—Example of a well in which pressure normalization successfully identified the straight-line trend of LF.

Significant and continued deviation from a ½ slope line on plot 4 can suggest deviation from transient LF. A deviation in the LF straight-line trend that remains deviated is an indication of a flow regime shift from the LF regime to the transition period. The slope of plot 4 was

recorded for each well with multiple slopes being recorded when clear deviations occurred indicating the transition period has begun. The transition flow regime is expected to be shown by a slope steeper than the LF slope range but less than two. The transition period is expected to last for many years due to the slow drainage nature of ultra-low permeability seen in shale reservoirs. A well that has existed in LF and begun the transition flow regime is illustrated in **Fig. 13**.

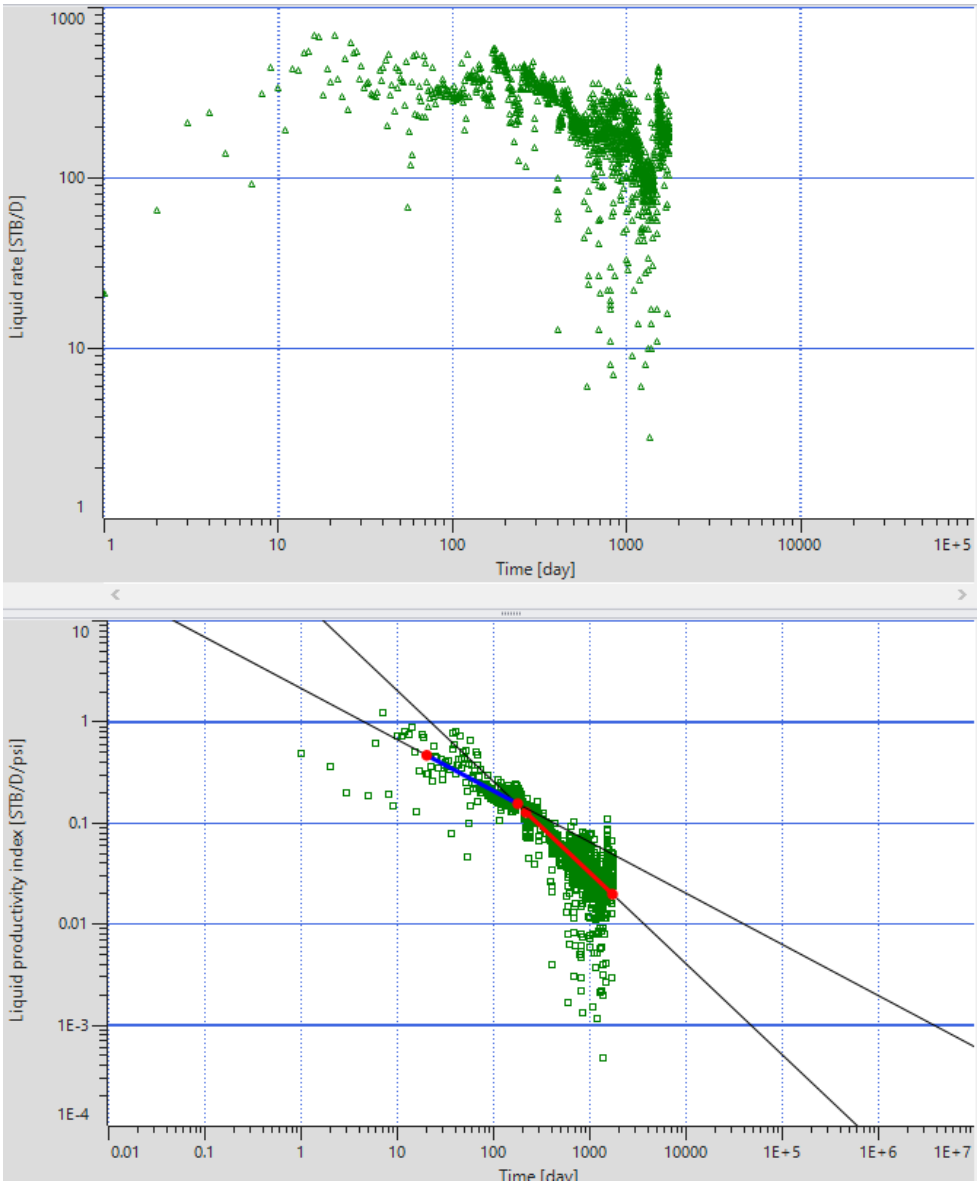

Fig. 13—Example of a well that has transitioned from LF.

Some wells seemed to skip the LF segment and immediately begin producing similar to wells in transition. Wells of this nature were assumed to be producing with partial fracture interference due to interconnected fracture networks creating a pseudo-boundary effect. This could cause wells to appear as if they are not producing linearly and have a PNR slope indicating they are in transition. Theoretically, shale wells in this region should produce in LF for many months or years, so it is safe to assume that these wells are encountering interference rather than transitional flow, as in **Fig. 14**. The well in this example has no indication of early time LF and the first (and only) identified segment has a best fit slope of 0.8, indicating it is affected by partial fracture interference.

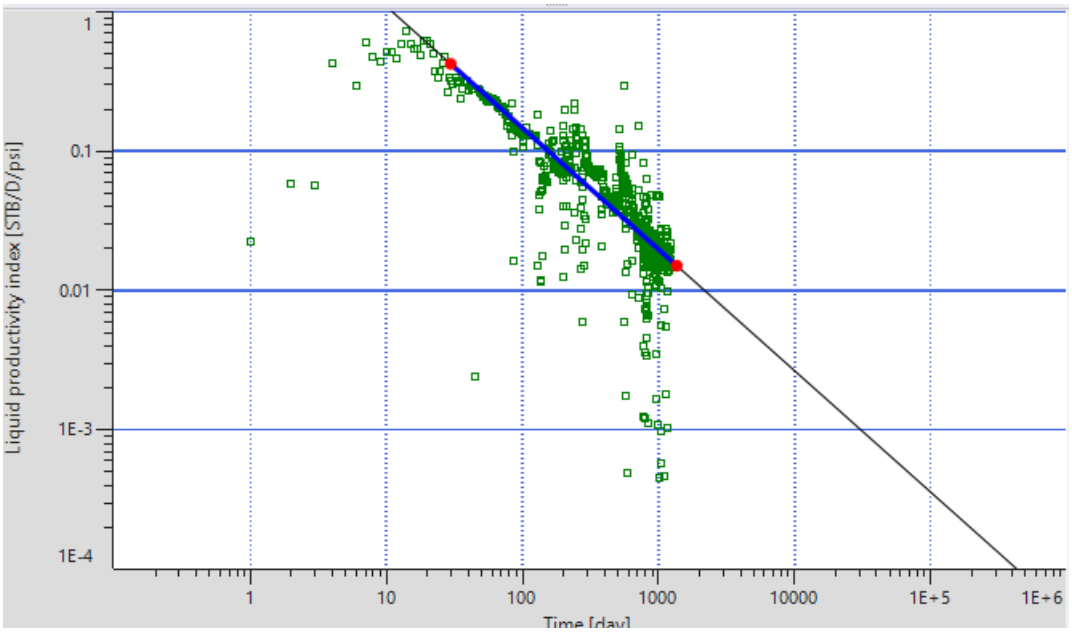

Fig. 14—Example of a well that is affected by partial fracture interference.

Complete fracture interference inducing a BDF effect may not be observed in production data during the life of an unconventional well. The BDF regime is characterized by a slope greater than two on diagnostic plot 4 but is not expected for the majority of these wells. The

ultra-low permeability of shale reservoirs, specifically in the Permian Basin, causes a prolonged period affected by boundaries as seen in the production data. Two wells in the data set were determined to be producing in the BDF regime. **Fig. 15** shows one of these wells exhibiting BDF. To confirm the presence of a transition or BDF, the segment of data in question was best fit with an Arps hyperbolic model to see if a transitional or BDF b-factor could be realistically and accurately fit to the data. If so, the flow regime identified was confirmed.

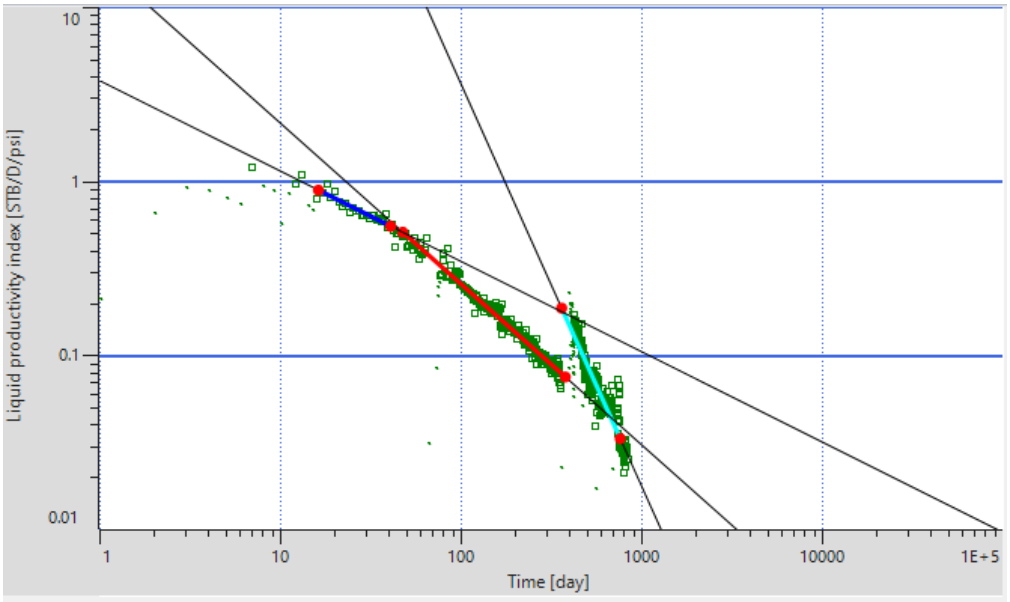

Fig. 15—Example of a well that exhibited LF, transition to BDF, and BDF.

Flow regime analysis was performed in its entirety for each well. The flow regimes were identified and the best fit slope and duration of each regime was recorded for each well. These slopes and durations were later used to generate multiple segment hyperbolic declines for each well.

Discussion of Results

The purpose of the flow regime identification portion of this analysis is to understand the long-term behavior of horizontal, multi-fractured, volatile oil shale wells in the Permian Basin and generate multi-segmented hyperbolic decline models for the wells based on identified flow regimes. Only the wells with "good" data (59/100 wells with correlated data that was not too noisy) are considered in this section of the study so as to draw valid conclusions on the typical behavior of these unconventional wells. The wells can further be divided into two different producing formations—Wolfcamp and Bone Springs.

The Wolfcamp group had 37 wells with good data. The average well in this data set had about 1,000 days of production. **Table 3** summarizes the flow regimes observed in this group. The majority (60%) of wells in this group were observed to be in LF with the other 40% exhibiting partial fracture interference without the presence of a LF segment. About 32% of the wells that exhibited LF to start began the transitional flow regime within the historical data period. Of the wells that illustrated transitional flow, the average duration of LF was about 230 days. The two wells that reached BDF within their production histories did so at 150 and 400 days, respectively. This analysis indicates that majority of wells producing from the Wolfcamp formation of the Permian Basin will produce in LF for more than 3 years without seeing the transition to BDF. It would be interesting future work to further study the impact of well spacing and operational conditions on the duration of LF.

Flow Regimes Observed	Number of wells	Percent of wells
LF	22	60%
↳ LF, Transition	↳ 7	↳ 32%
↳ LF, Transition, BDF	↳ 2	↳ 9%
No LF, Partial Fracture Interference	15	40%
Total Wells	**37**	-

Table 3—Summary of flow regime analysis for the Wolfcamp group.

The Bone Springs group had 22 wells with good data. The average well in this data set had about 1,800 days of production. **Table 4** summarizes the flow regimes in this group. The majority of these wells were observed to be in LF with only 27% of the wells exhibiting transitional flow within their historical data. The increase in average production time explains why a larger percent of the Bone Springs wells exhibited the transitional flow regime. With a longer producing time (i.e., more data), it should be expected that more wells should show indications of transitional flow. The wells that exhibited LF and a transition phase had a LF period that lasted about 625 days. This analysis indicates that majority of the wells producing in the Bone Springs formation of the Permian Basin will see fracture interference or transition to BDF within 5 years of production; however, wells are most likely to start production in LF. None of the wells in this reservoir showed indications of boundary effects due to complete fracture interference within the production history.

Flow Regimes Observed	Number of wells	Percent of wells
Bilinear Flow	1	5%
LF	15	68%
↳ LF, Transition	↳ 6	↳ 40%
No LF, Partial Fracture Interference	7	32%
Total Wells	**22**	-

Table 4—Summary of flow regime analysis for the Bone Springs group.

MULTI-SEGMENT HYPERBOLIC DECLINE MODELING

Application of Flow Regimes to MSH Model

The Multi-Segment Hyperbolic Method was implemented based on the flow regimes observed in the production data for each well. The model utilizes the Arps hyperbolic equation (Eq. 2). The b-factor used for each segment depends on the slope observed for each flow regime. For observed flow regimes, the b-factor was calculated using **Eq. 6**. For unobserved flow regimes, the b-factor was estimated using the ranges in **Table 5**. Using this constant b-factor for each segment, the model was fit to the data using linear regression by adjusting initial rate (q_i) and initial decline rate (D_i) to obtain the best fit decline curve.

$$b = \frac{1}{slope} \quad \text{.....(6)}$$

For the LF segment, a best-fit Arps hyperbolic decline was applied using a constant b-factor of 1.5 - 2.0. The LF segment lasts until the transition phase is detected. If no transition phase was detected, the LF was assumed to terminate at the end of history. Following LF, the transition period will bewas modeled using a b-factor of 0.5 – 1.5. If the transition period iswas observed in production data, the historical data was fitted to the model using the b-factor calculated from the slope of the PNR curve for the transition segment. If no transition region was detected during historical production, the b-factor was estimated using an average of the observed LF b-factor with the BDF b-factor (0.3). The transition period was assumed to continue up to a terminal decline rate of 10%. In common practice, this terminal decline rate marks the time at which the decline model switches to exponential decline. However, we believe that for

unconventional wells in particular, the data will continue to follow a hyperbolic decline model due to the presence of the boundary dominated flow regime. Although we expect that unconventional wells will enter boundary dominated flow segment towards the end of their life, there will not likely be BDF present in the historical data available, so we assumed that the wells enter BDF at a decline rate of 10%. For the BDF segment, the b-factor is assumed to be 0.3 for solution-gas-drive reservoirs (Fetkovich 1996). It is important that value of b during BDF be below one so that the estimated reserves are not overstated. The BDF segment will terminate at a total well life of 30 years so as to establish a comparable 30-year cumulative production estimate for each well.

Wells that exhibit partial fracture interference (no LF and calculated b-factor 0.5 to 1.5), were treated as similar to LF wells that had yet to undergo transition. These wells still have a declining b-factor, but the b-factor of the second segment is lower than if they were experiencing true LF at the start. In all cases where there is historical data available to fit the decline, the data were fit to the decline model. For cases where the forecast did not overlay historical data to obtain a best fit, *qi* and *Di* were initialized to match the flow rate and decline rate at the end of the previous segment. This ensures that the generated decline model is smooth without significant or unrealistic non-conformities in the curve. Table 5 summarizes the MSH model parameter distribution.

Flow Regime Segment	b	q_i, D_i	Segment Duration
Bilinear Flow	>=4.0	Best fit to data	To end of BLF
Linear Flow	1.5 - 2.0	Best fit to data	To end of LF or end of history
Partial Fracture Interference	0.5 – 1.5	Best fit to data	To end of interference or end of history
Transition to BDF	0.5 - 1.5	Best fit or initialized to previous segment	To terminal decline (10%)
BDF	0.3	Best fit or initialized to previous segment	To end of life (30 years)

Table 5—Summary of flow regimes segments and decline parameters used in the MSH method.

Modified Arps Modeling

To draw comparisons and conclusions for the MSH decline model, the modified Arps hyperbolic decline model was used. This modified model follows the hyperbolic equation, Eq. 2, like the MSH model. However, typically this model only uses a single b-factor to model the decline of the well before switching to an exponential decline (Eq. 3, b = 0) at a terminal decline rate. The modified Arps model decline types and parameters are summarized in **Table 6**. For this data set, this classic model was used for each well to compare the decline to the MSH method. The linear regression best fit curve was generated using Kappa Citrine by adjusting *qi*, *Di*, and *b* and applying an exponential decline at a terminal decline rate of 10%. **Fig. 16** shows an example comparison of the modified Arps model (yellow) and the MSH decline model (black).

Decline Type	*b*	*qi, Di*	Decline duration
Hyperbolic	0 – 2.0	Best fit to data	To terminal decline (10%)
Exponential	0	Initialized to previous segment	To end of life (30 years)

Table 6—Summary of decline types and parameters used in modified Arps method.

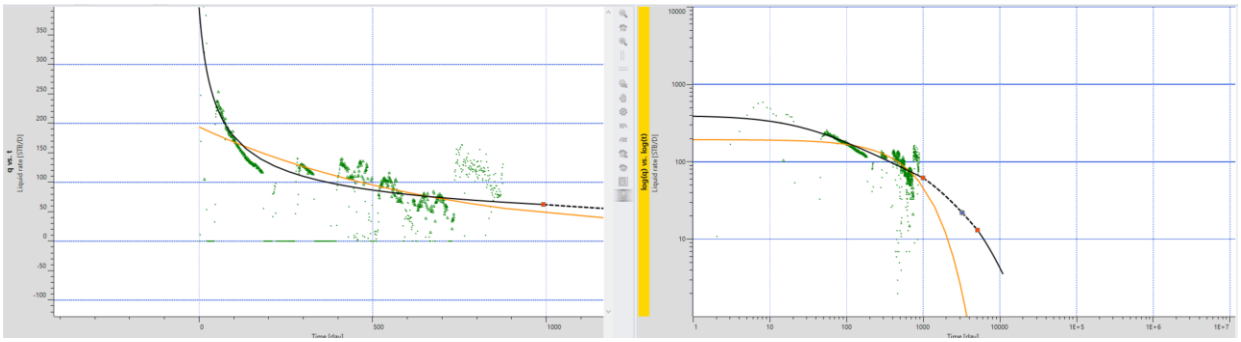

Fig. 16—Example comparison of the modified Arps model and MSH decline model.

Discussion

Case 1: Linear Flow

Well 34 is a good example of a well that is modeled using a LF segment to the end of its history. The flow regime analysis was performed using the diagnostic plots shown in **Fig. 17**. The pressure and rate data correlate well for the majority of production history and the data are not too noisy. The log-log plot of rate vs time shows a clear ½ slope trend through the data. The pressure normalized rate curve confirms this ½ slope throughout the life of the well to date. Therefore, we assumed that the well exhibited LF to the end of history (about 1,500 days). Using Eq. 6, the b-factor for the LF segment is 2.0. Since we do not see transitional flow in the historical data, an estimate of the b-factor was obtained using an average of the LF segment (2.0) and the BDF segment (0.3). The transition regime was modeled using a b-factor of 1.2. We assume that the transition segment begins at the end of history, since no historical data portrays transitional flow. The BDF segment begins at a terminal decline rate of 10%. This switch point was determined using the Kappa Citrine "switch to exponential" function that outputs a time to terminal decline following the modeling of the first two segments. Once the switch time was

determined, the BDF segment was set to begin at this time. For segments following LF, q_i and D_i were determined using the Citrine linear regression best fit function. The second segment is initialized at the q_f and D_f of the first segment. The third segment is initialized at the q_f of the third segment and a D_i of 10% since it begins at the terminal decline rate. **Fig. 18** depicts the parameters used to generate the MSH model for well 34. **Fig. 19** depicts the MSH decline model for well 34 on rate vs time and log-log rate vs time curves. The rate vs time graph is used to interpret the goodness of fit to the historical production. The log-log rate vs time graph is used to observe the decline model in its entirety as well as observed how the model fits the flow regimes observed in the log-log diagnostic plot used in the flow regime analysis. The transition segment is selected so as to show the start and end of each segment. The well exhibited LF to the end of history (4 years), followed by a transition to BDF that lasted about 3 years after the end of history, and ending with a BDF segment that was terminated at 30 years. This resulted in a 30-yr estimated ultimate recovery (EUR) of 0.462 MMSTB.

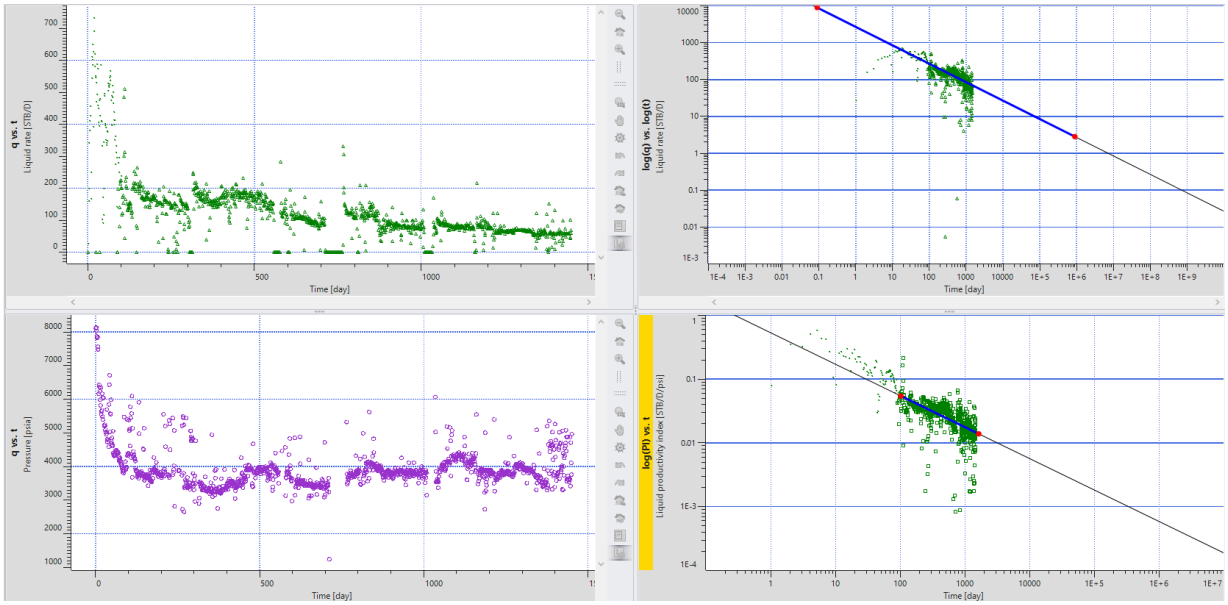

Fig. 17—Diagnostic plots used in the flow regime analysis of well 34.

Parameters		
Decline curve bounds		
Time stamp	10/13/2017 12:00:00 AM	
Hyperbolic Segment 1		
Segment type	Arps	
Tmin	0.00000	Year
Initial rate	☑ 597.114	STB/D
Decline parameter	☑ 7.55348	1/year
Initial tangent effective decline rate	99.9476	%/Year
Initial secant effective decline rate	75.0831	%/Year
b exponent	☐ 2.00000	
Exponential decline	☐	
Hyperbolic Segment 2		
Segment type	Arps	
Maintain initial rate with previous segment	☑	
Tmin	4.01530	Year
Initial rate	76.0431	STB/D
Decline parameter	☑ 0.15	1/year
Initial tangent effective decline rate	13.9292	%/Year
Initial secant effective decline rate	12.8839	%/Year
b exponent	☐ 1.20000	
Exponential decline	☐	
Hyperbolic Segment 3		
Segment type	Arps	
Maintain initial rate with previous segment	☑	
Tmin	6.80574	Year
Initial rate	54.1711	STB/D
Decline parameter	☑ 0.1	1/year
Initial tangent effective decline rate	9.51626	%/Year
Initial secant effective decline rate	9.38309	%/Year
b exponent	☐ 0.3	
Exponential decline	☐	
Abandonment		
Abandonment rate	9.31454	STB/D
Tmax	30.0000	Year
EUR	0.462749	MMSTB

Fig. 18—The MSH model parameters used to generate the decline for well 34.

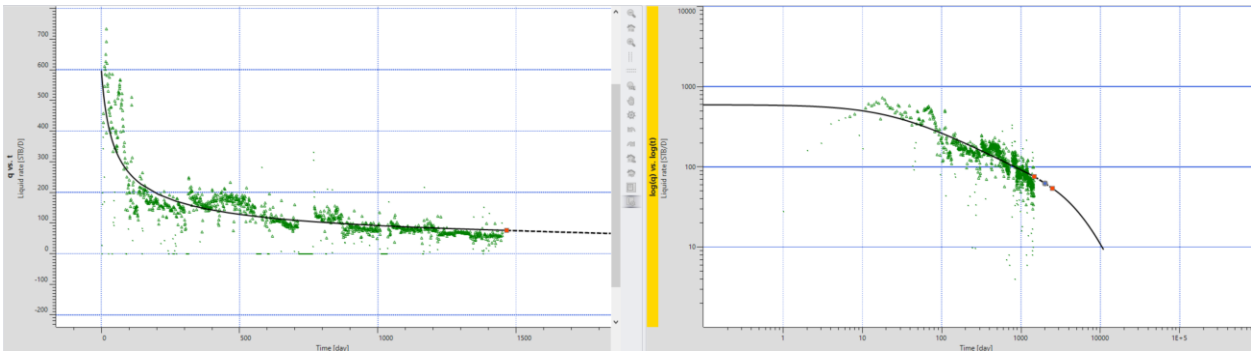

Fig. 19—The MSH model for Well 34.

Case 2: Linear Flow and Transition

Well 85 is a good example of a well that was modeled with both LF and transitional flow segments within the historical data. The flow regime analysis was performed using the diagnostic plots shown in **Fig. 20**. The pressure and rate data correlate well for the majority of production history and the data is not too noisy, aside from a noisy segment of rate data. Ignoring the clean-up period, the pressure normalized rate curve shows a ½ slope for about 350 days followed by a slope of 2, indicating transitional flow. Therefore, we can assume moving forward that the well exhibits LF ($b = 2.0$) for about 500 days then enters the transitional flow regime with a b-factor of 1.2. The BDF segment ($b = 0.3$) will begin at a terminal decline rate of 10%, which was determined to be about 6.6 years. The model parameters were best fit to the data or initialized to the previous segment, as in the previous example. **Fig. 21** depicts the parameters used to generate the MSH model for well 85. **Fig. 22** depicts the MSH decline model for well 85. The well exhibited LF for about 1.7 years followed by a transition to BDF that lasted about 5 years and ending with a BDF segment that was terminated at 30 years. This resulted in a 30-yr EUR of 0.265 MMSTB.

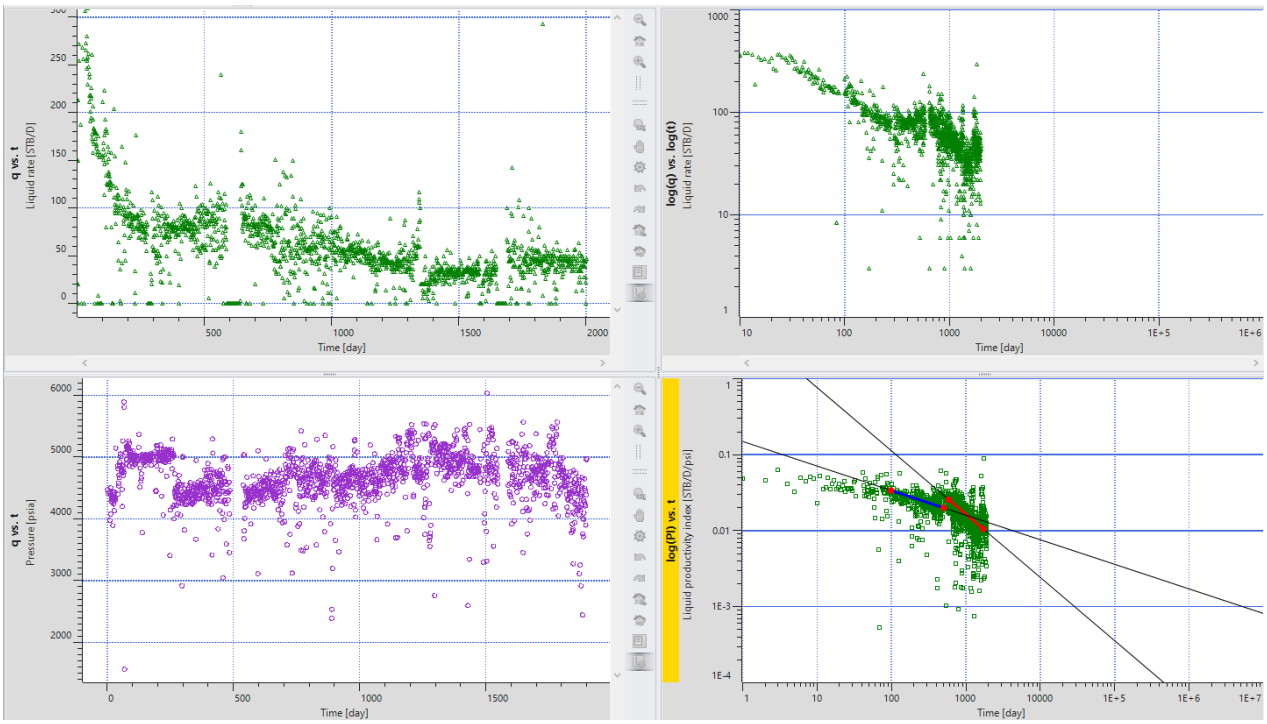

Fig. 20—Diagnostic plots used in the flow regime analysis of well 85.

Parameters		
Decline curve bounds		
Time stamp	4/16/2019 12:00:00 AM	
Hyperbolic Segment 1		
Segment type	Arps	
Tmin	0.00000	Year
Initial rate	☑ 343.597	STB/D
Decline parameter	☑ 7.40765	1/year
Initial tangent effective decline rate	99.9393	%/Year
Initial secant effective decline rate	74.8544	%/Year
b exponent	☐ 2.00000	
Exponential decline	☐	
Hyperbolic Segment 2		
Segment type	Arps	
Maintain initial rate with previous segment	☑	
Tmin	1.68978	Year
Initial rate	67.3403	STB/D
Decline parameter	☑ 0.25537	1/year
Initial tangent effective decline rate	22.5370	%/Year
Initial secant effective decline rate	19.9691	%/Year
b exponent	☐ 1.20000	
Exponential decline	☐	
Hyperbolic Segment 3		
Segment type	Arps	
Maintain initial rate with previous segment	☑	
Tmin	6.61619	Year
Initial rate	31.2796	STB/D
Decline parameter	☑ 0.1	1/year
Initial tangent effective decline rate	9.51626	%/Year
Initial secant effective decline rate	9.38309	%/Year
b exponent	☑ 0.3	
Exponential decline	☐	
Abandonment		
Abandonment rate	5.31875	STB/D
Tmax	30.0000	Year
EUR	0.26513	MMSTB

Fig. 21—The MSH model parameters used to generate the decline for well 85.

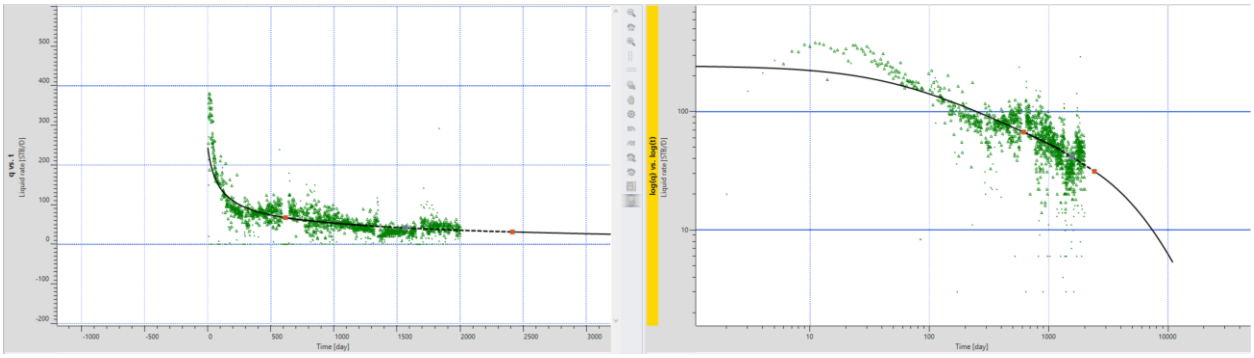

Fig. 22—The MSH model for well 85.

Case 3: Partial Fracture Interference Example

Well 59 is a good example of a well that is modeled with a partial fracture interference assumption. The flow regime analysis was performed using the diagnostic plots shown in **Fig. 23**. The pressure and rate data correlate well for the majority of production history and the data is not too noisy. Although the log-log plot indicates half slope trend, the pressure normalized rate curve shows a slope of 0.8 indicating the first segment will be fit with a b-factor of 1.3. This b-factor is outside the range expected for LF (1.5-2.0), thus it is assumed that this well is being influenced by partial fracture interference starting at early times. The transition segment for this model will begin at the end of history and the BDF segment (b = 0.3) will begin at a terminal decline rate of 10%, which is determined to be about 11 years. The model parameters were best fit to the data when available or initialized to the previous segment if not, as in previous examples. **Fig. 24** depicts the parameters used to generate the MSH model for Well 59. **Fig. 25** depicts the MSH decline model for Well 59. The well exhibited partial fracture interference for about 3 years followed by a transition to BDF that lasted about 8 years and ending with a BDF segment that was terminated at 30 years. This resulted in a 30-yr EUR of 0.512 MMSTB.

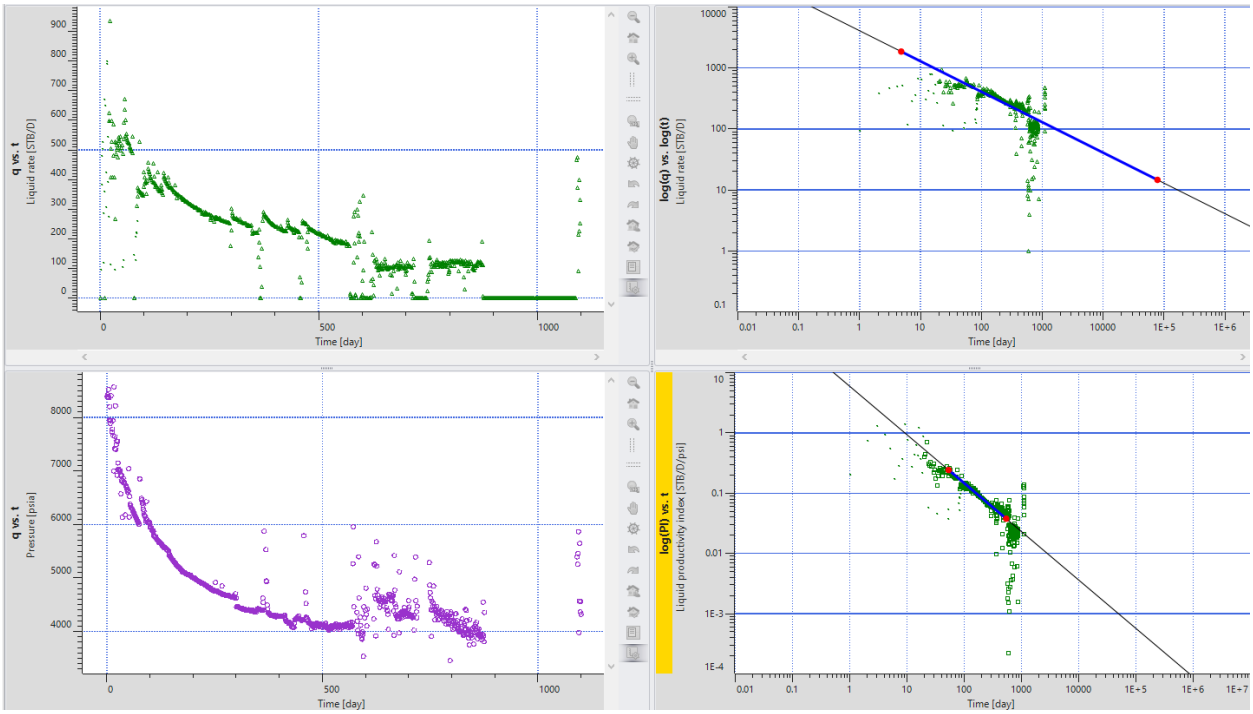

Fig. 23—Diagnostic plots used in the flow regime analysis of well 59.

Parameters		
Decline curve bounds		
Time stamp	10/27/2016 12:00:00 AM	
Hyperbolic Segment 1		
Segment type	Arps	
Tmin	0.00000	Year
Initial rate	☑ 703.678	STB/D
Decline parameter	☑ 2.52879	1/year
Initial tangent effective decline rate	92.0245	%/Year
Initial secant effective decline rate	67.3642	%/Year
b exponent	☐ 1.30000	
Exponential decline	☐	
Hyperbolic Segment 2		
Segment type	Arps	
Maintain initial rate with previous segment	☑	
Tmin	3.07658	Year
Initial rate	110.371	STB/D
Decline parameter	☐ 0.29	1/year
Initial tangent effective decline rate	25.1736	%/Year
Initial secant effective decline rate	22.9564	%/Year
b exponent	☐ 0.8	
Exponential decline	☐	
Hyperbolic Segment 3		
Segment type	Arps	
Maintain initial rate with previous segment	☑	
Tmin	11.1923	Year
Initial rate	29.3818	STB/D
Decline parameter	☐ 0.1	1/year
Initial tangent effective decline rate	9.51626	%/Year
Initial secant effective decline rate	9.38309	%/Year
b exponent	☐ 0.3	
Exponential decline	☐	
Abandonment		
Abandonment rate	6.61317	STB/D
Tmax	30.0000	Year
EUR	**0.512424**	**MMSTB**

Fig. 24—The MSH model parameters used to generate the decline for well 59.

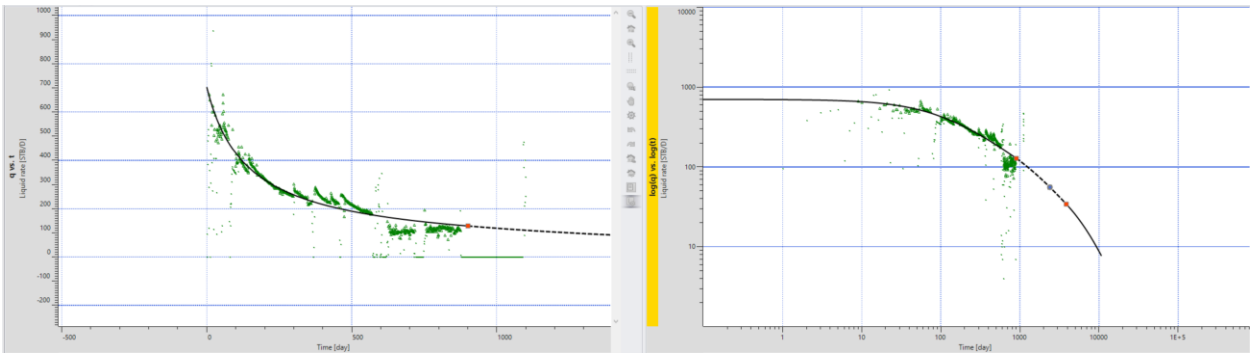

Fig. 25—The MSH model for well 59.

Case 4: LF, Transition to BDF, and BDF

Well 16 is a good example of a well that is best modeled with LF, transition to BDF, and BDF segments within its history. Only two wells in the data set were observed to be in BDF by the end of their production history. The flow regime analysis was performed using the diagnostic plots shown in **Fig. 26**. The pressure and rate data correlate well for the majority of production history and the data are not too noisy. The pressure normalized rate curve shows a near ½ slope trend, followed by a short transition segment and ending with a steep decline indicating BDF. The LF segment, the transition segment, and the BDF segment were modeled using b-factors of 1.8, 1.3, and 0.3, respectively. To confirm the flow regimes, a best fit decline was fit to each isolated segment using these b-factors to ensure that these data could be accurately modeled with these parameters. The gradual declining nature of this well is not characteristic of the steep decline often seen with wells in early time. Due to this initial gradual decline, the LF , we could not model the LF segment accurately. The decline model was started at the transition segment to best represent the decline profile of the well. The other model parameters were best fit to the data or initialized to the previous segment, as in previous examples. **Fig. 27** depicts the parameters used to generate the MSH model for well 16. **Fig. 28** depicts the MSH decline model for well 16.

The well exhibited LF for about 0.5 years followed by a transition to BDF that lasted about 1.5 years and ended with a BDF segment that was terminated at 30 years. This resulted in a 30-yr EUR of 0.241 MMSTB.

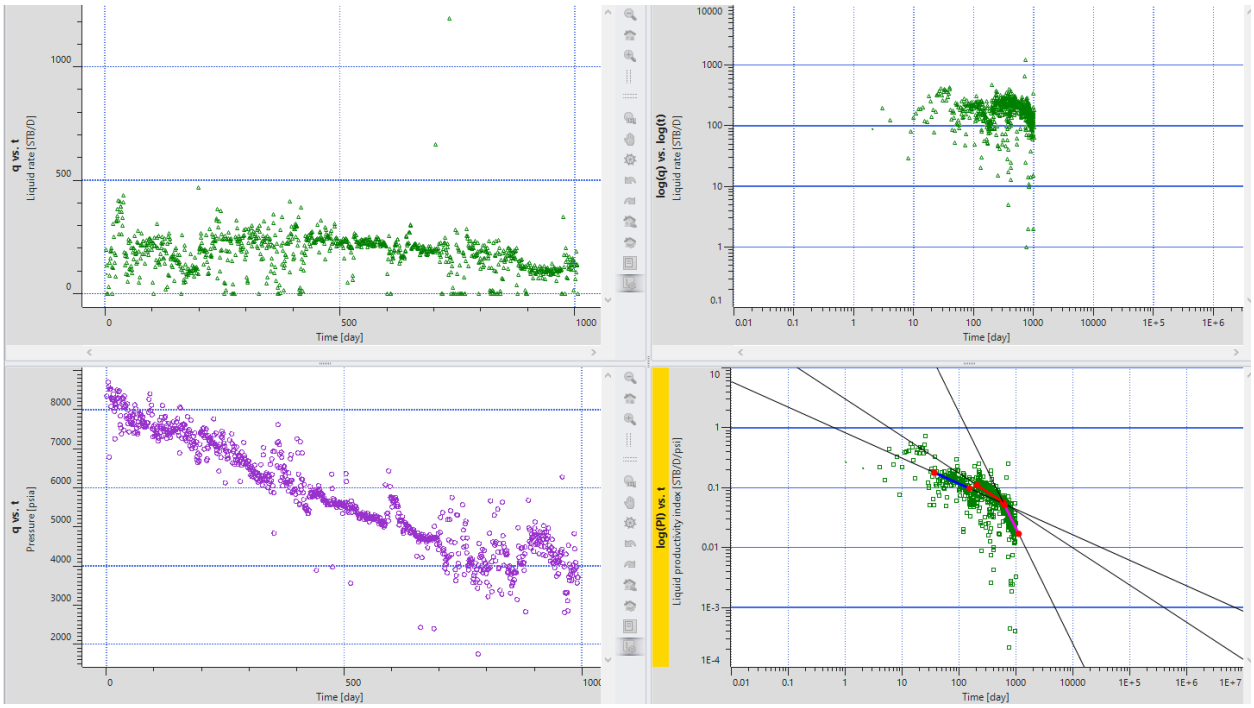

Fig. 26—Diagnostic plots used in the flow regime analysis of well 16.

Parameters		
Decline curve bounds		
Time stamp	7/26/2016 12:00:00 AM	
Hyperbolic Segment 1		
Segment type	Arps	
Tmin	0.547945	Year
Initial rate	☑ 249.414	STB/D
Decline parameter	☑ 0.156715	1/year
Initial tangent effective decline rate	14.5053	%/Year
Initial secant effective decline rate	13.2929	%/Year
b exponent	☐ 1.30000	
Exponential decline	☐	
Hyperbolic Segment 2		
Segment type	Arps	
Maintain initial rate with previous segment	☑	
Tmin	2.17176	Year
Initial rate	200.191	STB/D
Decline parameter	☑ 1.39091	1/year
Initial tangent effective decline rate	75.1151	%/Year
Initial secant effective decline rate	68.7280	%/Year
b exponent	☐ 0.3	
Exponential decline	☐	
Abandonment		
Abandonment rate	0.0428715	STB/D
Tmax	30.0000	Year
EUR	**0.241476**	**MMSTB**

Fig. 27—The MSH model parameters used to generate the decline for well 16.

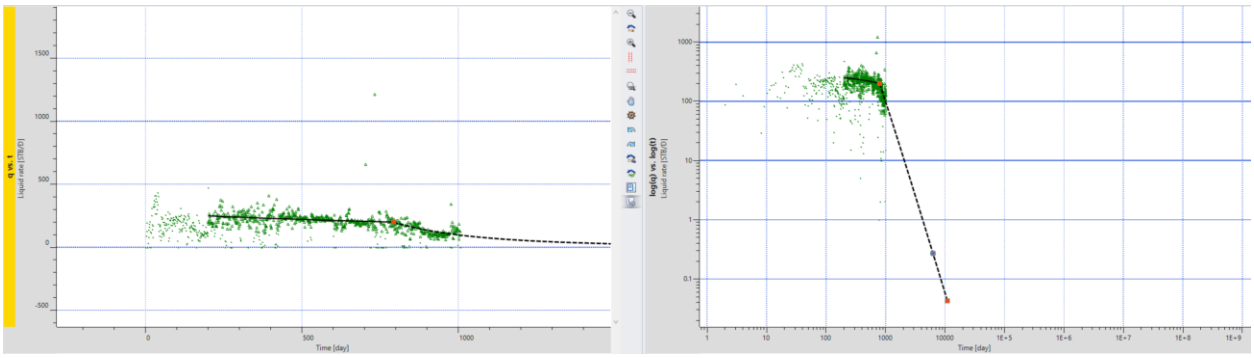

Fig. 28—The MSH model for well 16.

Case 5: Bilinear Flow

Well 79 is the only well in the data set that exhibited long-duration bilinear flow in its production history. The flow regime analysis was performed using the diagnostic plots shown in **Fig. 29**. The pressure and rate data correlate well for the majority of production history and the data are not too noisy. The pressure normalized rate curve shows a near 1/4 slope trend for nearly 1.5 years, followed by a LF ½ slope. The BLF segment was modeled with a b-factor of 4.0 while the LF segment was modeled using a b of 2.0. The terminal decline switch point was estimated to be immediately following the end of history, so no transition phase was modeled. The model will switch to BDF (b = 0.3) at the end of history. To confirm the flow regimes, a best fit decline was modeled to each isolated segment using these b-factors to ensure that the rate data could be accurately modeled with these parameters. The other model parameters were best fit to the data or initialized to the previous segment, as in previous examples. **Fig. 30** depicts the parameters used to generate the MSH model for well 79. **Fig. 31** depicts the MSH decline model for well 79. The well exhibited BLF for about 1.5 years followed by LF that lasted about 4 years and ending with a BDF segment that was terminated at 30 years. This resulted in a 30-yr EUR of 0.298 MMSTB.

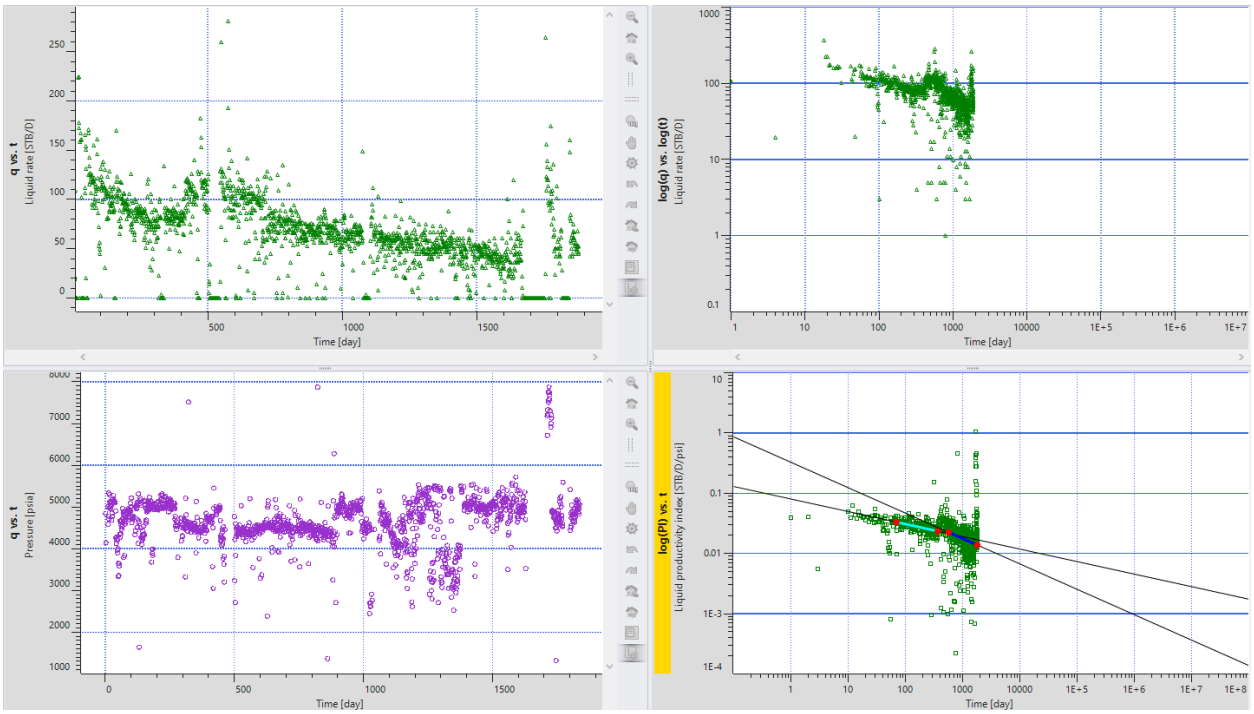

Fig. 29—Diagnostic plots used in the flow regime analysis of well 79.

Parameters		
Decline curve bounds		
Time stamp	4/16/2019 12:00:00 AM	
Hyperbolic Segment 1		
Segment type	Arps	
Tmin	0.00000	Year
Initial rate	☑ 141.193	STB/D
Decline parameter	☑ 2.27336	1/year
Initial tangent effective decline rate	89.7034	%/Year
Initial secant effective decline rate	43.8964	%/Year
b exponent	☐ 4.00000	
Exponential decline	☐	
Hyperbolic Segment 2		
Segment type	Arps	
Maintain initial rate with previous segment	☑	
Tmin	1.26948	Year
Initial rate	75.0246	STB/D
Decline parameter	☑ 0.2136	1/year
Initial tangent effective decline rate	19.2329	%/Year
Initial secant effective decline rate	16.2938	%/Year
b exponent	☐ 2.00000	
Exponential decline	☐	
Hyperbolic Segment 3		
Segment type	Arps	
Maintain initial rate with previous segment	☑	
Tmin	5.21733	Year
Initial rate	45.7729	STB/D
Decline parameter	☑ 0.1	1/year
Initial tangent effective decline rate	9.51626	%/Year
Initial secant effective decline rate	9.38309	%/Year
b exponent	☑ 0.3	
Exponential decline	☐	
Abandonment		
Abandonment rate	7.17605	STB/D
Tmax	30.0000	Year
EUR	**0.298175**	**MMSTB**

Fig. 30—The MSH model parameters used to generate the decline for well 79.

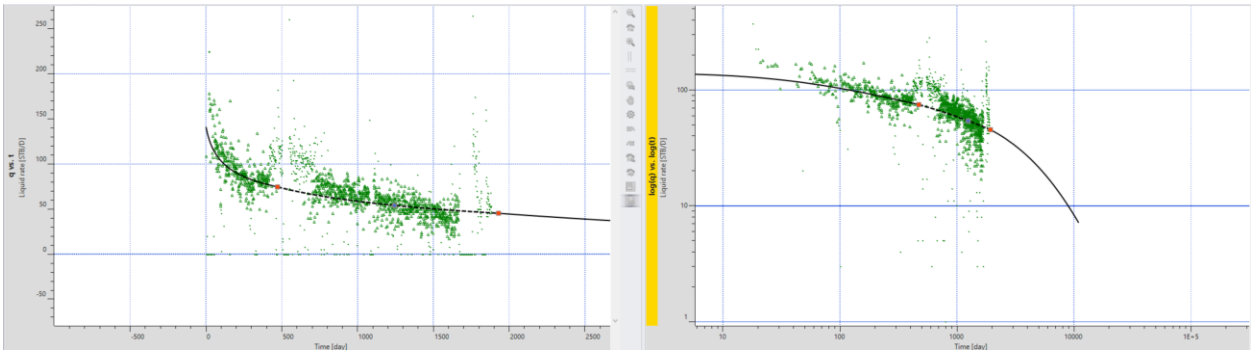

Fig. 31—The MSH model for well 79.

Results

Model comparisons, as in Fig. 28, were performed and accumulated for individual wells and each reservoir to understand how the MSH model compares to the modified Arps method. The decline parameters, decline profile, and 30-year EUR's are compared for each well in the entire data set and Wolfcamp and Bone Springs reservoirs, individually.

The model parameters for all good data are compared in **Table 7**. The first segment, identified as LF (b = 1.5 – 2.0) in 37 wells and as fracture interference (no LF and b = 0.5 – 1.5) in 22 wells, was modeled using P90, P50, and P10 b-factors of 1.1, 1.5, and 2.0, respectively. Of the 13 wells that met an end to linear flow within the available production history, the distribution of linear flow duration was 0.2, 1.1, and 2.4 years for P90, P50, and P10, respectively. This indicates that, although in a majority of wells, the end of linear flow did not occur within the 5.5 years of production history available in this data set, wells that did reach the end of linear flow, did so after about one year of production. The second segment, identified as transition to BDF (b = 0.5 – 1.5), was modeled using P90, P50, and P10 b-factors of 0.7, 0.9, and 1.2, respectively. The BDF segment was always modeled using a b of 0.3, so there is no distribution of values. The Wolfcamp and Bone Springs formations had similar parameter

distributions as in the entire field. These distributions can be seen in **Tables 8 and 9**. The modified Arps method used best fit b parameters as listed in Tables 6 through 8. The b-factors varied from 0 to 2 for the entire field, with half of the wells fit best with a b of 1.3.

Probability	MSH		Modified Arps
	1st segment b	2nd segment b	1st segment b
P90	1.1	0.7	0
P50	1.5	0.9	1.3
P10	2	1.2	2

Table 7—The MSH and modified Arps b-factor distributions for the entire good data set.

Probability	MSH		Modified Arps
	1st segment b	2nd segment b	1st segment b
P90	0.9	0.6	0
P50	1.5	0.9	1.2
P10	2	1.2	2

Table 8—The MSH and modified Arps b-factor distributions for the Wolfcamp group.

Probability	MSH		Modified Arps
	1st segment b	2nd segment b	1st segment b
P90	1.2	0.8	0.8
P50	1.7	0.9	1.4
P10	2	1.2	1.9

Table 9—The MSH and modified Arps b-factor distributions for the Bone Springs group.

In general, the MSH model 30-year EUR was greater than for the modified Arps model. The overall distribution of EUR's for the MSH and modified Arps methods using all of the good data can be compared in the histograms in **Fig. 32**. The mean of the EUR's for only good data came out to 0.601 MMSTB and 0.567 MMSTB for the MSH and Arps models, respectively.

This suggests the Arps model generally underestimates reserves for multi-fracture, horizontal, volatile oil shale wells. This conclusion is confirmed when looking at the cumulative distribution of the two methods in **Fig. 33**. There were 15 cases out of the 59 "good" data wells analyzed that indicated the Arps EUR was greater than the MSH EUR. In almost all of these cases, the MSH model analysis indicated the well was best modeled using the well interference flow regime (b = 0.5 – 1.5), but the modified Arps model was best fit with a higher b-factor closer to 2.0. Since a b-factor of 2.0 is characterized by a sharp initial decline and much more gradual decline over time, these higher b-factors would yield a higher EUR in general. Since the MSH model in these cases started with a lower b-factor, and used a declining b-factor with each subsequent decline segment, we would expect that the EUR would be lower for the MSH model in cases like this. This is one of the shortcomings of the modified Arps model. The subjectivity with which rate data can be fit using multiple declines using a variety of parameters is the most significant source of uncertainty associated with the Arps model. Application of flow regime analysis to multiple segments of Arps decline is one way to ensure modeling using the Arps method is less subjective and more representative of the production data.

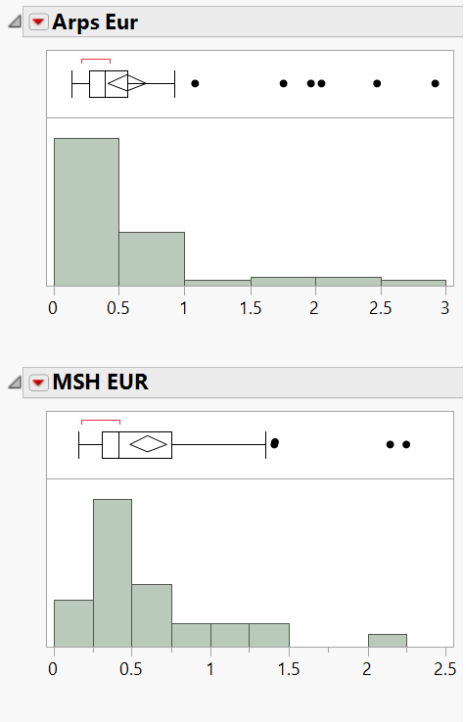

Fig. 32—Comparing modified Arps and MSH model EUR distributions for all the good data.

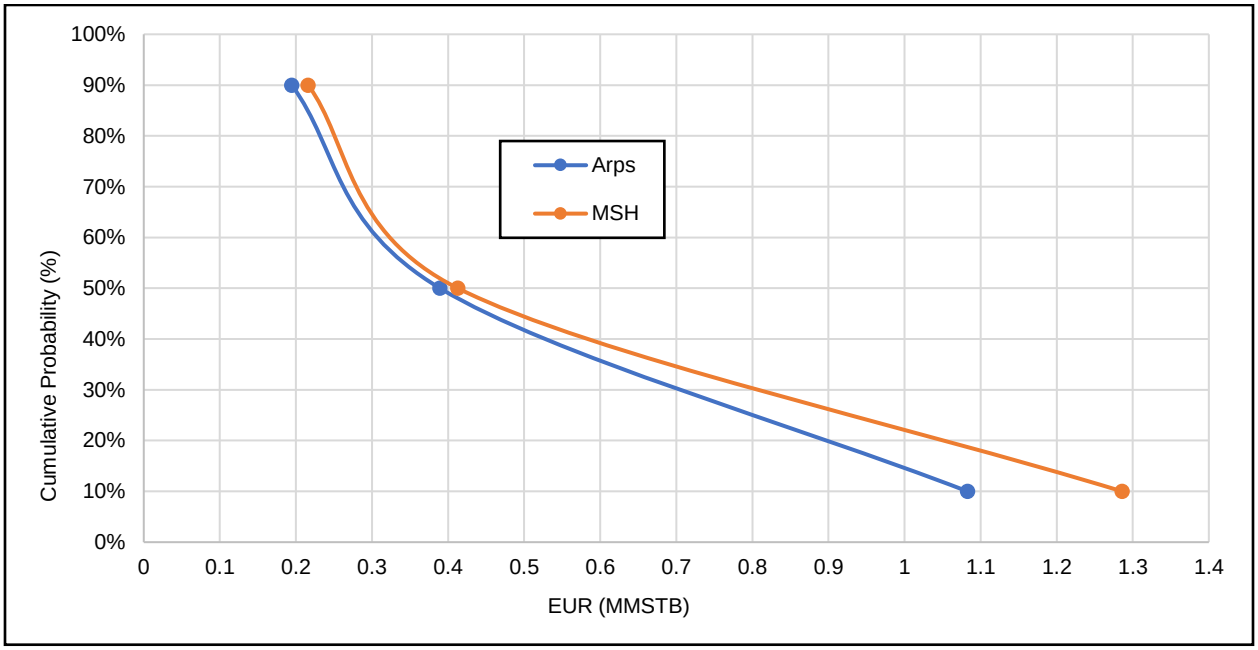

Fig. 33—Comparison of P10, P50, P90 values of the MSH and Arps methods for the all good data.

For the Wolfcamp group, the distribution of EUR's can be seen in **Fig. 32**. The means for the Wolfcamp Arps EUR and MSH EUR are 0.711 and 0.740 MMSTB, respectively. The probability distributions illustrating the P10, P50, and P90 values of EUR's are shown in **Fig. 35**. The significant outliers observed in the Arps EUR distribution cause the P90 values for the Arps distribution to be greater than the P90 values estimated for the MSH method. Each of these outliers exhibits the well interference characteristics mentioned in section X. The MSH decline curve in these cases uses a b-factor that is less than the best fit b-factor used in the modified Arps method, causing the EUR estimate to be greater for the Arps model. Removal of these outliers would generate a more realistic P90 EUR distribution. In general, the modified Arps model estimates smaller reserves for the Wolfcamp group than the MSH model estimates.

The P10, P50, and P90 EUR distributions were used to generate Wolfcamp type wells, or possible range of well declines expected to be observed for the field. These type wells can be used to predict long term well behavior early in the life of a new well producing from the Wolfcamp formation. The EUR's were used to select wells that could be categorized as P10, P50, and P90 type wells. These values and the type wells selected are summarized in **Table 10** and illustrated in **Figs. 36 through 38**.

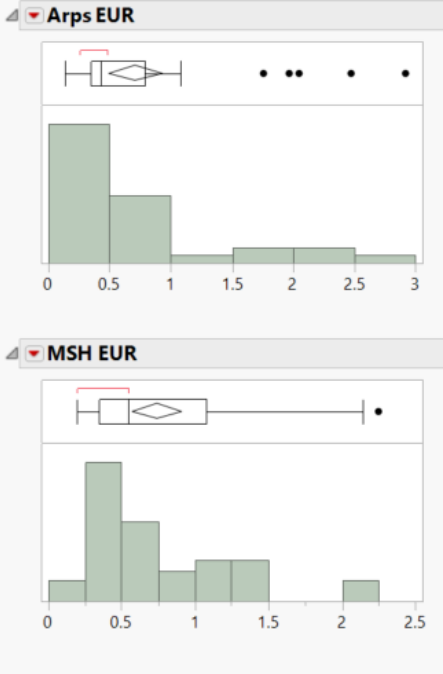

Fig. 34—Comparing Arps and MSH model EUR distributions for the Wolfcamp group.

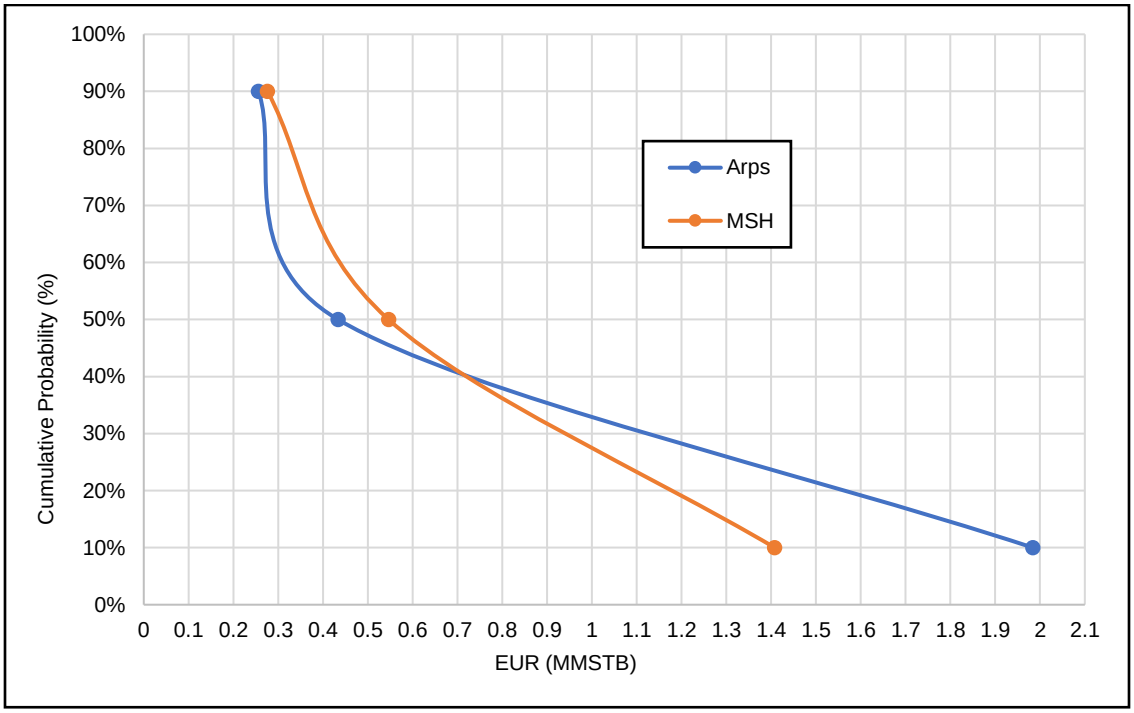

Fig. 35—Comparison of P10, P50, P90 values of the MSH and Arps methods for the Wolfcamp group.

Probability	Modified Arps		MSH	
	EUR, MMSTB	Well Selected	EUR, MMSTB	Well Selected
P90	0.256	44	0.276	10
P50	0.433	21	0.546	55
P10	1.984	48	1.408	53

Table 10—Summary of P10, P50, and P90 EUR's and type wells selected for the Wolfcamp group.

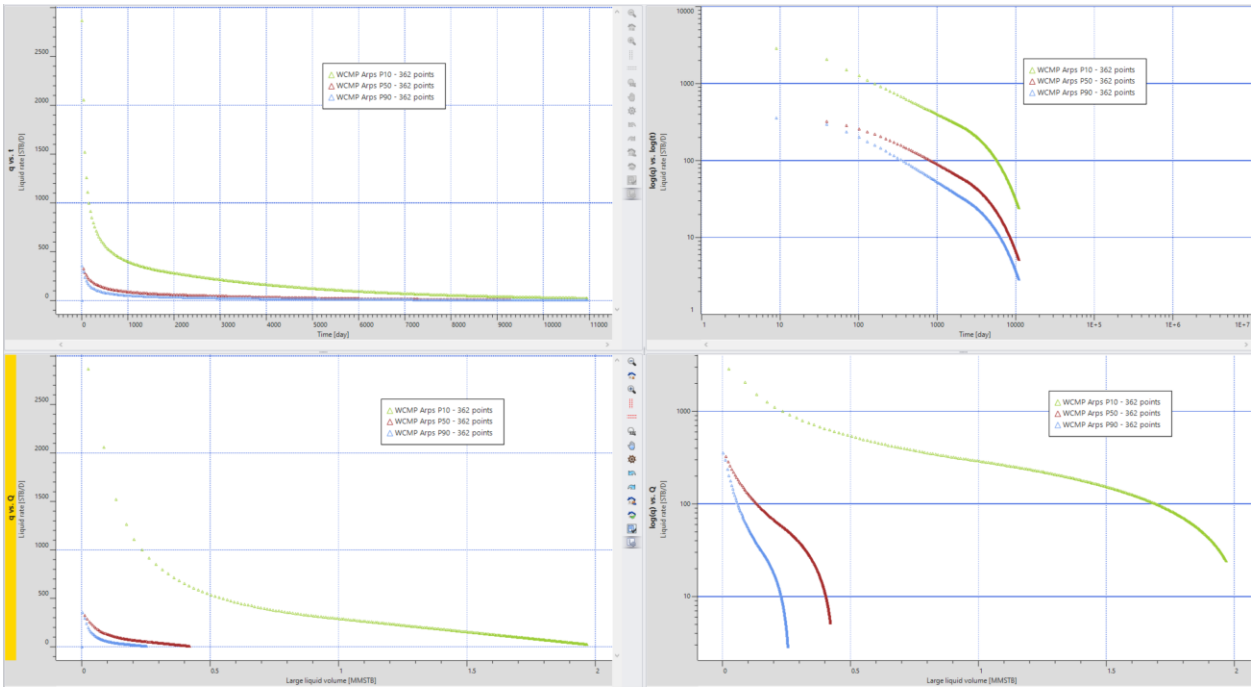

Fig. 36—Modified Arps method type wells for the Wolfcamp group.

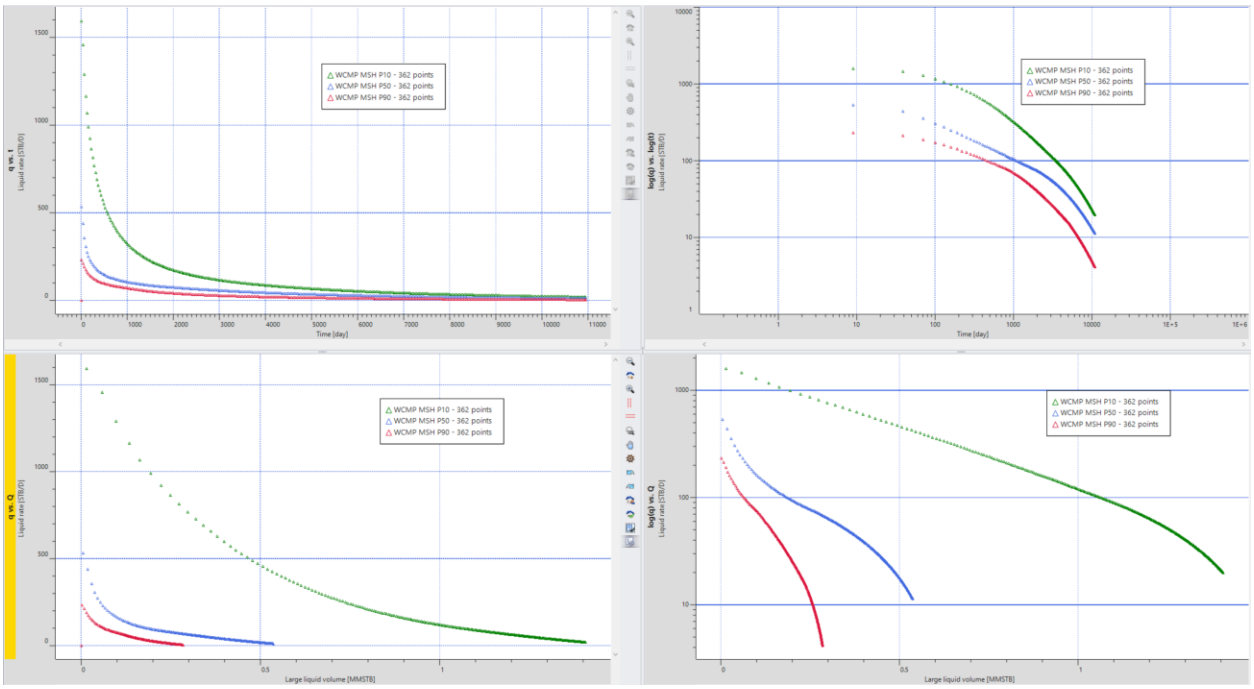

Fig. 37—MSH method type wells for the Wolfcamp group.

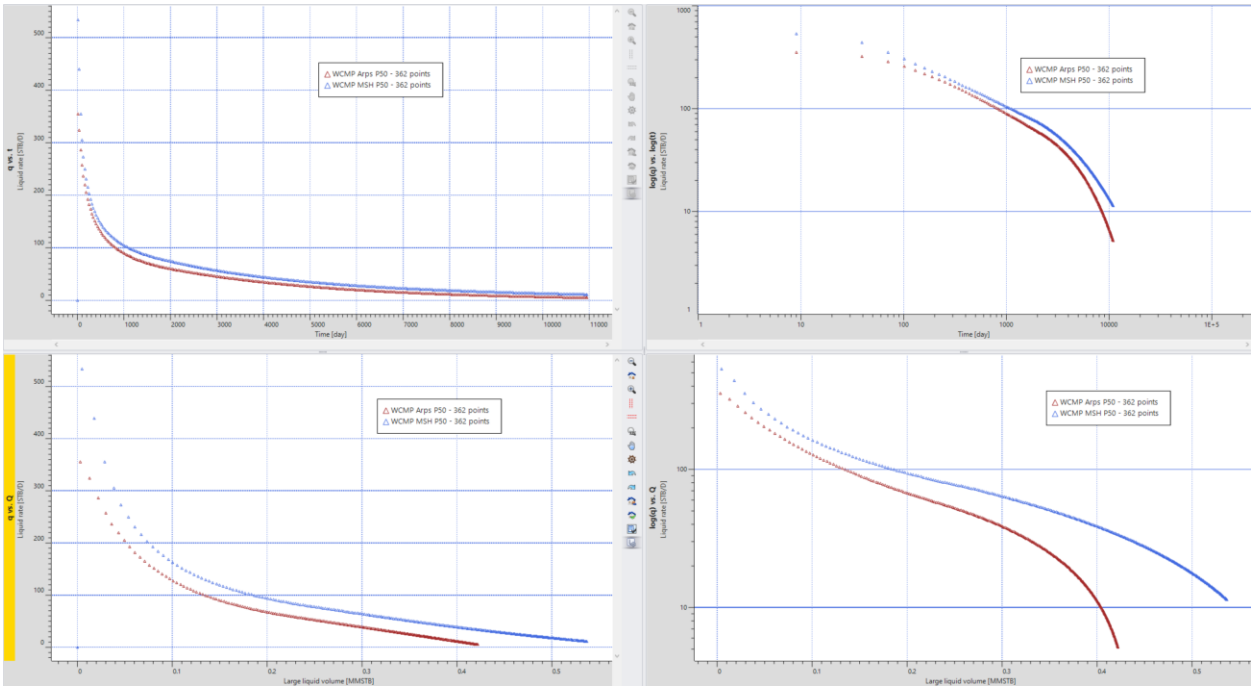

Fig. 38—Comparison of P50 Arps (red) and P50 MSH (blue) type wells for the Wolfcamp group.

For the Bone Springs group, the distribution of EUR's can be seen in **Fig. 39**. The means for the Bone Springs Arps EUR and MSH EUR are 0.324 and 0.368 MMSTB, respectively. The cumulative distributions illustrating the P10, P50, and P90 values of EUR's are shown in **Fig. 40**. For this reservoir, the EURs in the MSH distribution are greater than in the Arps distribution for all probabilities. This is an indication that the modified Arps model underestimates reserves for the Bone Springs group.

The P10, P50, and P90 EUR distributions are used to generate Bone Springs type wells. These type wells can be used to accurately predict long term well behavior early in the life of a new well producing in the Bone Springs formation. The EUR's were used to select wells that could be categorized as P10, P50, and P90 type well. These values and the type wells selected are summarized in **Table 11** and illustrated in **Figs. 41 through 43**.

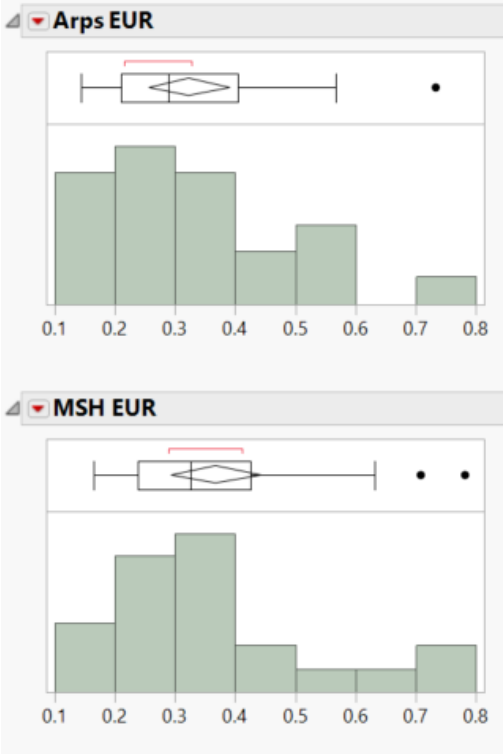

Figure 39—Comparing Arps and MSH model EUR distributions for the Bone Springs group.

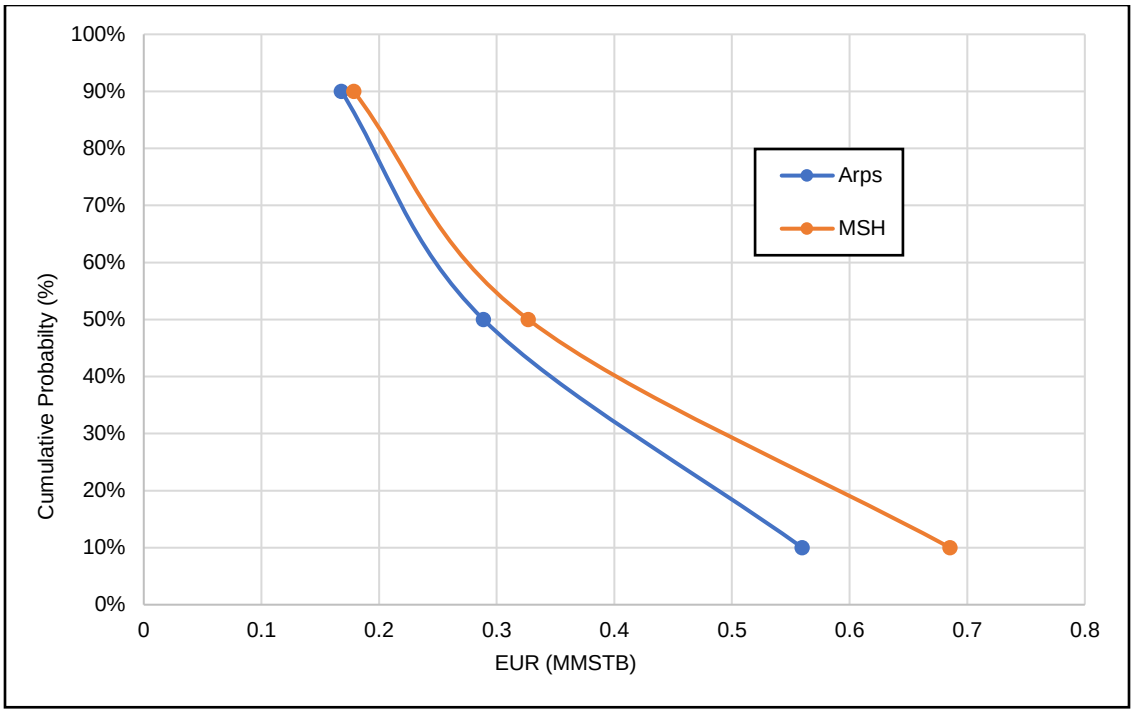

Fig. 40—Comparison of P10, P50, P90 values of the MSH and Arps methods for the Bone Springs group.

Probability	Modified Arps		MSH	
	EUR, MMSTB	Well Selected	EUR, MMSTB	Well Selected
P90	0.168	43	0.179	82
P50	0.289	87	0.327	38
P10	0.560	80	0.685	80

Table 11—Summary of P10, P50, and P90 EUR's and type wells selected for the Bone Springs group.

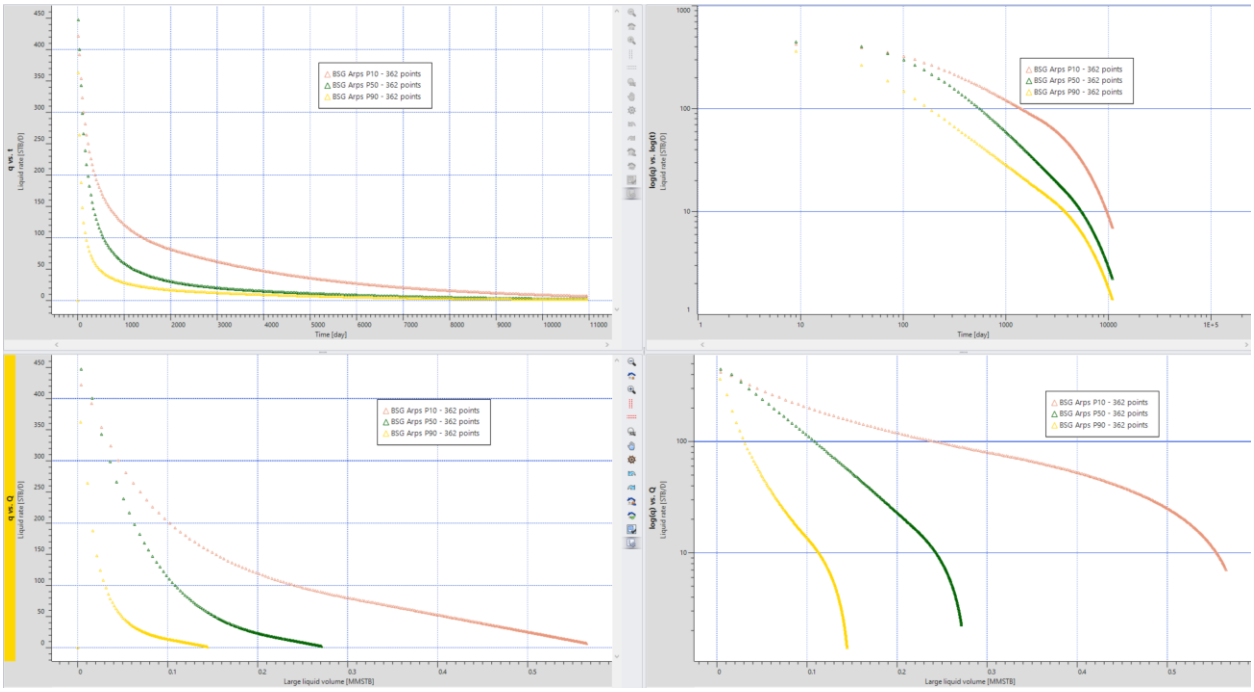

Fig. 41—Modified Arps method type wells for the Bone Springs group.

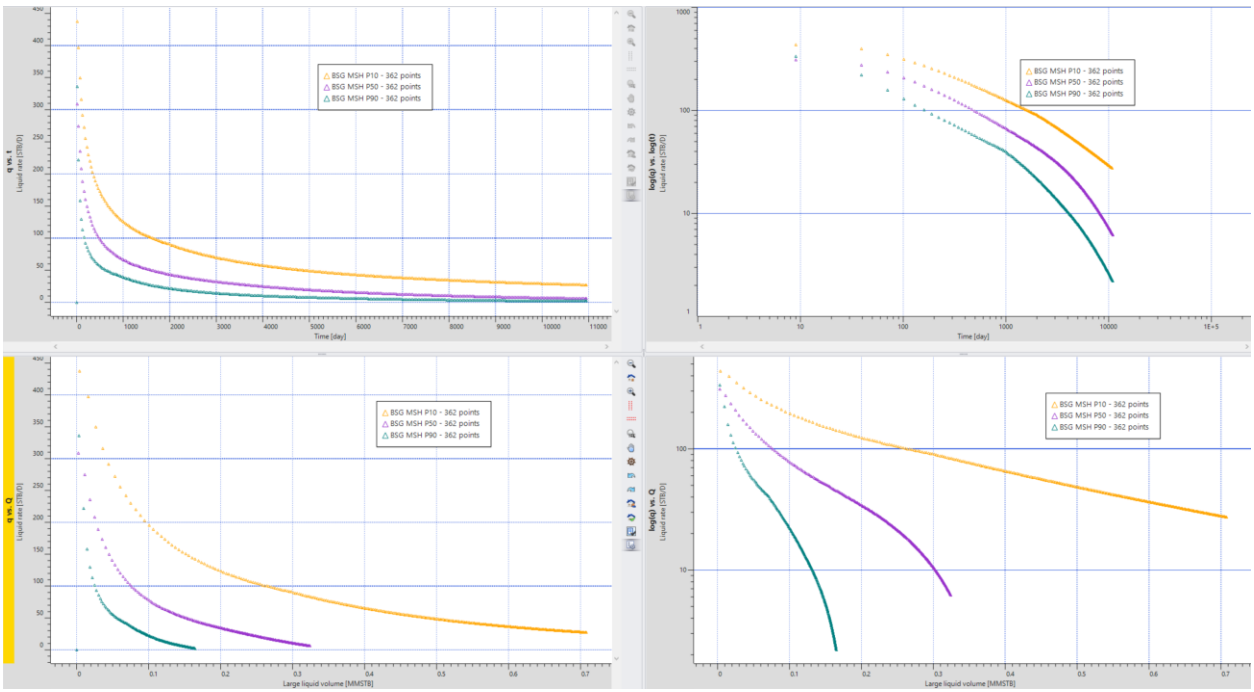

Fig. 42—MSH method type wells for the Bone Springs group.

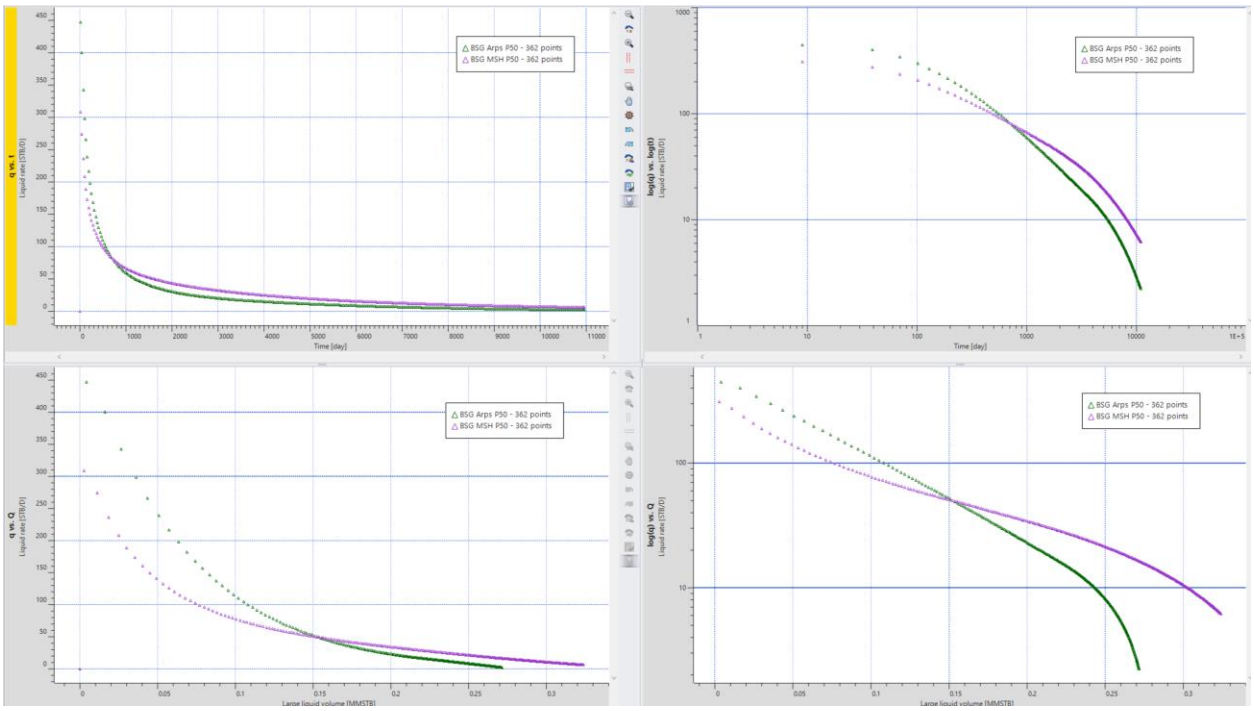

Fig. 43—Comparison of P50 Arps (green) and P50 MSH (purple) type wells for the Bone Springs group.

CONCLUSIONS

The Multi-Segment Hyperbolic Method proved to be a viable method to model the decline of unconventional wells. The transient nature of ultra-low permeability volatile oil shale reservoirs causes a sharp decline initially followed by a gradual decline over time that is best modeled with multiple Arps hyperbolic segments identified with distinct flow regimes rather than the dual-segment modified Arps model most often used in industry today. Modeling multiple segments based on flow regimes observed in production data adds a degree of ingenuity and robustness to the widely accepted Arps model. This study has highlighted the following key insights and conclusions on modeling horizontal, multi-fractured, volatile oil, shale wells in the Permian Basin.

Shale Well Behavior

- The log-log PNR vs time plot serves as a better diagnostic tool than the lo-log rate vs time plot in identifying flow regimes in unconventional wells using production data.
- Noise and lack of data correlation can cause inaccuracy in flow regime identification and decline curve analysis.
- Early time fracture clean-up and shut-ins impact data noise and flow regime analysis, but the effect is lessened by using the PNR plot.
- Shale wells in the Permian Basin typically exhibit LF for multiple years.
- Wells experiencing LF can be best modeled using an Arps b-factor of 1.5 – 2.0.
- Partial fracture interference impacts a significant portion (~44%) of Permian wells.

- Wells experiencing partial fracture interference can be modeled best without a linear flow segment and using an Arps b-factor of 0.5 – 1.5.
- About 1/4th of shale wells in the Permian Basin begin the transition to BDF within 3 years of production.
- Wells transitioning to BDF can be best modeled using a b-factor of 0.5-1.5 post LF.
- A vast majority (97%) of shale wells in the Permian Basin do not exhibit BDF within the first 5.5 years of production.
- Wells experiencing BDF can be best modeled using a b-factor of 0.3, as Fetkovich (1996) derived for solution-gas-drive volatile oil reservoirs.
- It is possible but not likely for a shale well to exhibit bilinear flow early in the life of the well.
- Wells producing in bilinear flow, although very unlikely, can be best modeled using a b-factor greater than or equal to 4.
- Based on flow regime analysis, the b-factor will decline over time as the well transitions from LF to BDF.

Modeling Shale Wells

- The Arps model is too subjective and inconsistent for modeling complex unconventional well behavior.
- The MSH model based on identified flow regimes is a robust method to model the decline of unconventional wells.
- The modified Arps model typically underestimates reserves when compared to the MSH model.

- P10, P50, and P90 type wells can be accurately generated using the MSH method to improve unconventional well forecasting.
- The Wolfcamp reservoir typically generates more prolific (higher EUR) wells than the Bones Springs reservoir.

NOMENCLATURE

b = decline exponent factor

BDF = boundary dominated flow

BLF = bilinear flow

D = decline parameter

D_f = final decline parameter

D_i = initial decline parameter

EUR = estimated ultimate recovery

LF = linear flow

MSH = multi-segment hyperbolic

p = pressure

P10 = value at confidence level 10%

P50 = value at confidence level 50%

P90 = value at confidence level 90%

p_i = initial reservoir pressure

PNR = pressure normalized rate

p_{wf} = flowing bottom-hole pressure

q = production rate

q_f = final production rate

q_i = initial production rate

t = time

Δp = pressure differential

REFERENCES

AbdelMawla, A., Hegazy, M. 2015. Important Considerations for Reserves Estimation in Unconventional Resource Plays. Paper SPE-177444-MS. Presented at Abu Dhabi International Petroleum Exhibition and Conference held in Abu Dhabi, UAE, 2015.

Arps, J.J. 1944. Analysis of Decline Curves. Trans. AIME 160: 228–247.

Chaudhary, N., Lee, W.J. Detecting and Removing Outliers in Production Data to Enhance Production Forecasting. 2016. Paper SPE-179959-MS presented at APE/AIEE Hydrocarbon Economics and Evaluation Symposium held in Houston, TX.

Duong, Anh N.: "An Unconventional Rate Decline Approach for Tight and Fracture-Dominated Gas Wells," paper SPE 137748, presented at the Canadian Unconventional Resources & International Petroleum Conference held in Calgary, Alberta, Canada, 19–21 October 2010.

Fairhurst, Bill, Hanson, Mary, Reid, Frank, Pieracacos. 2012. Wolfbone Play Evolution, Southern Delaware Basin: Geologic Concept Modifications That Have Enhanced Economic Success. Search and Discovery Article #10412 adapted from presentation given at AAPG 2012 Southwest Section Meeting in For Worth, TX.

Fetkovich, M.J., Fetkovich, E.J., Fetkovich, M.D. 1996. Useful Concepts for Decline-Curve Forecasting, Reserve Estimation, and Analysis. Paper SPE-28628-PA presented at SPE ATCE, New Orleans, 1994.

Ilk, D., Jenkins, C. D., Blasingame, T.A. 2011. Production Analysis in Unconventional Reservoirs—Diagnostics, Challenges, and Methodologies. Paper SPE-144376 presented at SPE NA Unconventional Gas Conference and Exhibition in The Woodlands, TX.

Ilk, D., Rushing, J.A., Perego, A.D. et al. 2008. Exponential Vs. Hyperbolic Decline in Tight Gas Sands: Understanding the Origin and Implications for Reserve Estimates Using Arps' Decline Curves. SPE-116731-MS. Presented at the SPE Annual Technical Conference and Exhibition, Denver, Colorado, USA, 21–24 September.

Jeyachandra, B., Sharma, A, Dwivedi, P., Gupta, S. 2016. Reservoir Flow Regime Assisted Multi-Segment Production Forecasting. Paper SPE-180982-MS presented at the SPE Argentina Exploration and Production of Unconventional Resources Symposium held in Buenos, Aires, Argentina.

Kanfar, M.S. and Alkouh, A.B. 2014. Bilinear Flow in Shale Gas Wells: Fact or Fiction? Paper SPE-171669-MS presented at SPE/CSUR Unconventional Resources Conference held in Calgary, Alberta, Canada.

Kupchenko, C.L., Gault, B.W., Mattar, L. 2008. Tight Gas Production Performance Using Decline Curves. Paper SPE 114991 presented at the CIPC/SPE Gas Technology Symposium 2008 Joint Conference in Calgary, Alberta, Canada.

Lacayo, J., Lee, W. J. 2014. Pressure Normalization of Production Rates Improves Forecasting Results. Paper SPE-168974-MS. Presented at SPE Unconventional Resources Conference held in The Woodlands, TX.

Makinde, I., Lee, W. J. 2016. Forecasting Production of Shale Volatile Oil Reservoirs Using Simple Models. Paper SPE-179964-MS presented at SPE/IAEE Hydrocarbon Economics and Evaluation Symposium held in Houston, TX.

Olson, Bradley, Elliott, Rebecca, Matthews, Christopher. 2019. Fracking's Secret Problem—Oil Wells Aren't Producing as Much as Forecast. *The Wall Street Journal.* (in press; published online on 2 January 2019). https://www.wsj.com/articles/frackings-secret-problemoil-wells-arent-producing-as-much-as-forecast-11546450162

Spivey, J.P., Frantz, J.H., Williamson, J.R., Sawyer, W.K. 2001. Applications of the Transient Hyperbolic Exponent. Paper SPE-71038.

Tang, Hewei, Chai, Zhi, Killough, John. 2017. Paper URTEC 2668100 presented at Unconventional Resources Technology Conference held in Austin, TX.

Varma, S., Tabatabaie, S. H., Ewert, J., Mattar, L. 2018. Variation of Hyperbolic-b-parameter for Unconventional Reservoirs, and 3-Segment Hyperbolic Decline. URTEC-2892966. Presented at URTEC in Houston, TX.

Wattenberger, R. A., El-Banbi, A. H., Villegas, M., et al., (5–8 April) 1998. Production Analysis of Linear Flow into Fractured Tight Gas Wells. Paper SPE-39931-MS presented at the SPE Rocky Mountain Regional/Low-Permeability Reservoirs Symposium, Denver, Colorado, USA.